Volume 16
Number 47
21 December 2025
Pages 5029-5118

Polymer Chemistry

rsc.li/polymers

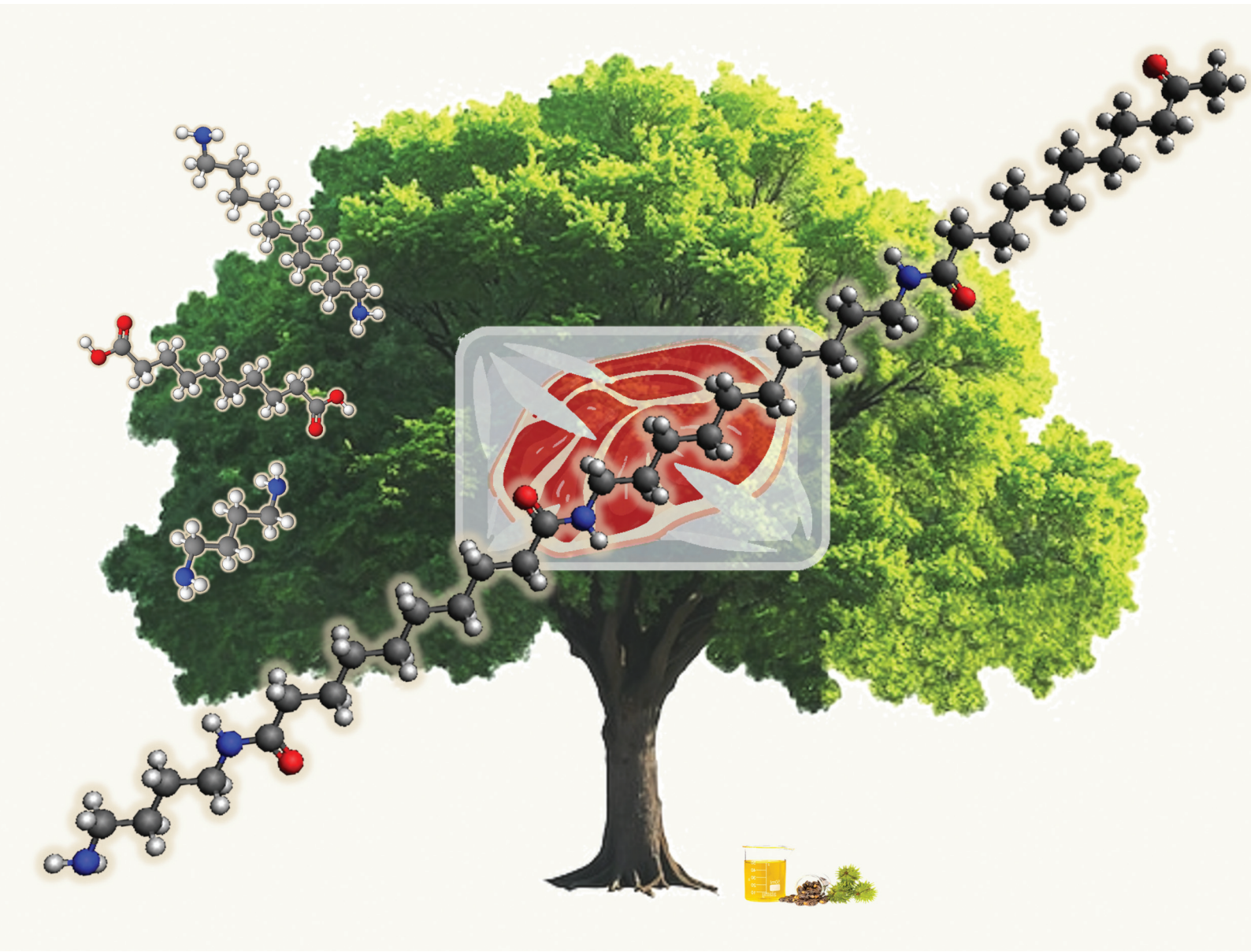

ISSN 1759-9962

ROYAL SOCIETY OF CHEMISTRY

PAPER
Sergio Torres-Giner *et al.*
Synthesis and characterization of copolyamide 1010/410 with varying putrescine contents for meat packaging applications

15 YEARS ANNIVERSARY

Polymer Chemistry

ROYAL SOCIETY OF CHEMISTRY

PAPER

View Article Online
View Journal | View Issue

Check for updates

Cite this: *Polym. Chem.*, 2025, **16**, 5040

Synthesis and characterization of copolyamide 1010/410 with varying putrescine contents for meat packaging applications

Marta Pacheco-Romeralo, [a] Eva Hernández-García, [a] Antxon Martínez de Ilarduya, [b] Ronak Janani,[c] Chris Sammon [c] and Sergio Torres-Giner *[a]

Acting on the Bioeconomy strategy, this study has developed fully bio-based copolyamide 1010/410 (PA1010/410) from "nylon salts" derived from renewable putrescine, decamethylenediamine, and sebacic acid monomers. Different fully bio-based copolyamides were synthetized by the polycondensation reaction of nylon 1010 salt with 12.5, 25, and 37.5 mol% of nylon 410 salt. Thereafter, the resultant PA1010/410 grades were shaped into 150-μm films by thermo-compression and characterized. Results showed that the putrescine content presents a strong influence on the molecular weight, crystallinity and, hence, thermal, mechanical, and barrier properties of PA1010/410. In particular, it was observed that the introduction of nylon 410 contents at 25 and 37.5 mol% resulted in PA1010/410 grades in the 2–3 × 10^4 g mol^{-1} range, with a crystallinity as low as ~15%. Interestingly, these copolyamide compositions led to transparent films melting at nearly 180 °C, being highly ductile with elongation at break of up to 130% and improved barrier to oxygen with a permeability as low as 5.3 × 10^{-19} m^3 m m^{-2} Pa^{-1} s^{-1}. These green nylons were finally applied as lid films in trays to preserve beef meat, and were shown to successfully extend food shelf life beyond those of current commercial monolayer solutions based on petrochemical polymers, thereby showing their potential for use in sustainable food packaging.

Received 31st July 2025,
Accepted 5th November 2025

DOI: 10.1039/d5py00766f

rsc.li/polymers

Open Access Article. Published on 15 1447. Downloaded on 18/07/47 09:14:27 .
This article is licensed under a Creative Commons Attribution 3.0 Unported Licence.

1. Introduction

The use of biopolymers as packaging materials to replace petrochemical polymers is becoming an emerging trend due to their natural and renewable origin and biodegradability.[1] Biopolymers used as food packaging materials mainly include naturally occurring polymers, for example, carbohydrates and proteins, and aliphatic polyesters obtained from monomers derived from natural resources. These biopolymers present film-forming capacities and sufficient physical properties to maintain food quality and increase shelf life of foodstuffs.[2] However, naturally occurring polymers, such as starch or cellulose, tend to show weak mechanical strength and high sensitivity to moisture, hindering their widespread industrial adoption.[3,4] Furthermore, the main limitation of using biopolyesters in food packaging is their low barrier properties that control the exchange of water and aroma vapors and oxygen gas.[5] Therefore, the use of these biopolymers in the form of monolayers is currently restricted to low-performance applications, such as plastic bags, lid films, or food-contact disposables.[6]

Polyamides have long been recognized as one of the major engineering thermoplastics, finding several applications in food packaging.[7] Among their exceptional properties, homo- and copolyamides habitually show good processability, high mechanical and thermal resistance as well as balanced barrier performance against water vapor and oxygen.[8] Although polyamides have traditionally been synthesized from petroleum derived diacids and diamines, some partially and fully bio-based polyamides have also been developed recently using renewable monomers, endowing comparable physical properties to their petrochemical counterparts.[9] Thus, bio-based aliphatic polyamides, also referred as "green nylons", can offer the advantage of using biomass and the unique potential of carbon neutrality so that these perfectly align with the Bioeconomy principles.[10] As one of the most promising green nylons, polyamide 1010 (PA1010) can be produced by polycon-

[a]*University Institute of Food Engineering—FoodUPV, Universitat Politècnica de València (UPV), Camino de Vera s/n, 46022 Valencia, Spain.*
E-mail: storresginer@upv.es
[b]*Departament d'Enginyeria Química, Universitat Politècnica de Catalunya (UPC), Barcelona School of Industrial Engineering (ETSEIB), Diagonal 647, Barcelona, 08028, Spain*
[c]*School of Engineering and Built Environment, Sheffield Hallam University, City Campus, Howard Street, Sheffield SI 1WB, UK*

This journal is © The Royal Society of Chemistry 2025

Open Access Article. Published on 15 1447. Downloaded on 18/07/47 09:14:27 .
This article is licensed under a Creative Commons Attribution 3.0 Unported Licence.

densation reaction using 1,10-decamethylenediamine and sebacic acid, which can be both obtained from castor oil, a natural and renewable industrial raw material.[11] The resultant fully bio-based PA1010 has proven to result especially attractive for food packaging applications that require transparency, high thermal stability, balanced mechanical strength and ductility, low water uptake, and moderate oxygen barrier.[12]

All types of polyamides consist of amide groups separated by alkane segments of different length, which results in different amide concentration per polymer chain. Whereas the polar amide groups contribute to their mechanical strength, thermal resistance, and chemical stability, the long-chain aliphatic methylene (CH_2) groups provide mechanical flexibility and water resistance. Indeed, the methylene-to-amide (CH_2/CONH) ratio, in combination with the chain symmetry, determines the final properties of polyamides.[13] Thus, lower CH_2/CONH ratios, that is, higher CONH densities per unit length of chain, increase hydrogen bond density and reduce segmental inter-chain mobility of the CH_2 groups in the polymer backbone, which favor hydrogen bonding and organization of polyamide chains into more ordered crystalline regions. Consequently, even-even polyamides with low CH_2/CONH ratios present high thermal transitions and mechanical strength that may not be optimal for flexible packaging applications where materials with a low sealing initiation temperature (SIT) and high ductility are required.[14] In the particular case of PA1010, its CH_2/CONH ratio is 9, resulting in a melting temperature (T_m) of approximately 200 °C and with moderate flexibility, which makes its films difficult to seal and with a non-optimal performance for certain food packaging applications.[15]

Accordingly, within the food packaging area, it currently becomes necessary to design and modify the chemical structure of PA1010 to both improve sealing and reduce energy consumption during processing as well as increase ductility of its films. Copolymerization represents a common modification method in polymer chemistry and thus the polyamide properties can be adjusted according to the final application by changing both the types of comonomers and their ratios.[16] Furthermore, the new monomers or units being introduced to reconstruct the chemical structure are nowadays expected to be biomass- or bio-originated, which can preserve the bio-based characteristics of the polyamide. In this regard, some diamines used to produce polyamides are naturally occurring substances, or they can be produced by microbial biosynthesis, for example by decarboxylation of the lysine or ornithine amino acids, such as 1,4-diaminobutane (putrescine) and 1,5-diaminopentane (cadaverine).[17,18] For instance, Koning and coworkers[19] developed semicrystalline copolyamides from renewable sebacic acid, diaminoisoidide, and putrescine, exhibiting tuneable polarities and T_m values ranging from 152 °C to 246 °C. Similarly, Rwei *et al.*, synthesized novel semicrystalline copolyamides from renewable dimethyl adipate (an ester of adipic acid), putrescine, and sebacic acid, showing that their T_m and glass transition temperature (T_g) values decreased from 211.0 °C to 164.0 °C and 66.6 °C to 43.5 °C, respectively.[20] To the best of our knowledge, there was no report on the synthesis and characterization of aliphatic bio-based copolyamides produced from "nylon salts" derived from renewable putrescine, 1,10-decamethylenediamine, and sebacic acid monomers. This monomer combination offers the possibility to develop novel green nylons with sufficient molecular weight and tailor-made performance.

In the view of interest of our previous study dealing with the synthesis and food packaging application of PA1010,[12] it is described herein the polycondensation reaction at different contents of nylon 1010 and nylon 410 salts to produce copolyamide 1010/410 (PA1010/410). Then, the different copolyamide grades were chemically analyzed and thermo-compressed into films and, thereafter, fully characterized to ascertain the putrescine content effect on their crystallinity, thermal, optical, mechanical, and barrier properties. Finally, the application of the newly developed bio-based copolyamide films was validated by packaging minced beef and assessing food shelf life for a period of cold storage of 11 days.

2. Materials and methods

2.1. Materials

1,10-Diaminodecane or 1,10-decamethylenediamine (98%) with CAS No. 646-25-3 was purchased from TCI Chemicals at CYMIT Química S.L. (Barcelona, Spain). Renewable sebacic acid (99%) with CAS No. 111-20-6 and putrescine (99%) with CAS No. 110-60-1 were obtained from Sigma-Aldrich S.A. (Madrid Spain). Absolute ethanol (EtOH), 2,2,2-trifluoroethanol (TFE), deuterated chloroform ($CDCl_3$), 1,1,1,3,3,3-hexafluoro-2-propanol (HFIP), and D-limonene were also obtained from Sigma-Aldrich S.A. Magnesium nitrate ($Mg(NO_3)_2$) and diphosphorus pentoxide (P_2O_5) were provided by Panreac Química S.L.U (Castellar del Vallés, Spain). Commercial polypropylene (PP), used as the benchmark material for the food shelf-life tests, was supplied by LyondellBasell (Houston, Texas, USA) as Moplen HP501L. This homopolymer, also developed for injection- and compression-molding applications, has a density of 0.90 g cm^{-3} (23 °C) and a melt flow index (MFI, 230 °C and 2.16 kg) of 6 g per 10 min. Minced beef meat was purchased from a local supermarket (Mercadona, Valencia, Spain). The microbiological media Violet Red Bile Agar (VRB) for total coliform counts, Plate Count Agar (PCA) for total viable counts, and peptone water were provided by Scharlab S.L. (Barcelona, Spain). Man, Rogosa and Sharpe agar (MRS) for lactic acid bacteria counts was purchased from Lankem-Labbox (Barcelona, Spain).

2.2. Polyamide synthesis

Synthesis of the bio-based polyamides was performed in two steps, that is, preparation of a "nylon salt" and subsequent melt polycondensation of the salt in a glass reactor. This methodology has proven to be effective to control the dicarboxylic acid/diamine ratio and avoid premature chain termination.[12]

Preparation of "nylon salts". "Nylon salts" are the organic precursors used in the polymerization reaction to ensure stoi-

Open Access Article. Published on 15 1447. Downloaded on 18/07/47 09:14:27 .
This article is licensed under a Creative Commons Attribution 3.0 Unported Licence.

chiometry between the diamines and diacids. Nylon 1010 salt was prepared following our previous optimized conditions.[12] To this end, a solution of 1,10-decamethylenediamine (1.05 eq.) in EtOH (43% wt/wt) was added drop by drop to a solution of sebacic acid (1 eq.) in EtOH (10% wt/wt) at 55 °C. During the addition, a precipitate formed, and the mixture was stirred for 1 h at 55 °C. Then, the mixture was cooled down on ice for 1 h. After that, the supernatant liquid was removed, and the precipitate was washed with EtOH at room temperature for 2 h. Finally, the salt was filtered and washed with EtOH until the pH was neutral. The white powder was recrystallized from an EtOH/water mixture (10 : 1 vol/vol) and dried at 60 °C in a vacuum oven (VaciotermT, JP Selecta S.A., Barcelona, Spain) for 8 h. A similar procedure was used to prepare the nylon 410 salt. A solution of putrescine (1.01 eq.) in EtOH (43% w/w) was added dropwise to a solution of sebacic acid (1 eq.) in EtOH (10% w/w) at 55 °C. The precipitate formed during the addition was stirred for 2 h at 55 °C and the mixture was cooled on ice for 1 h. After that, the supernatant liquid was removed and the precipitate was washed with EtOH, stirring it at room temperature for 2 h. Finally, the salt was filtered and washed with EtOH until the pH was neutral. The white powder was recrystallized from an EtOH/water mixture (20 : 1 vol/vol) and dried at 60 °C for 8 h in a vacuum oven (VaciotermT).

Melt polycondensation. PA1010 was synthesized from its nylon salt by melt polycondensation in the same glass polymerization unit and following similar conditions reported previously.[12] Briefly, 30 g of nylon 1010 salt was placed in a 100-mL glass jacketed reactor connected to a heating station (Huber Pilot ONE CC-304B, Peter Huber Kältemaschinenbau AG, Offenburg, Germany) based on an immersion bath with high temperature control. A mechanical stirrer and a *Vigreaux* condensation column with a glass distillation adapter were attached to the reactor through a 5-neck lid. The reactor was closed, and the system was purged with an inert nitrogen (N_2) atmosphere at a flow-rate of 200 mL min^{-1} for 1 h, while the salt was stirred at 30 rpm. The gas outlet was sealed, and the system was left under positive pressure during a heating ramp from room temperature to 230 °C at a heating rate of 3.3 °C min^{-1}. Once the reaction temperature was reached, the N_2 gas outlet was opened with a flow-rate of 50 mL min^{-1} to drag the reaction by-products. Then, stirring was increased to 75 rpm and the reaction was left for 3 h. Finally, the reactor system was allowed to cool down under an inert atmosphere to room temperature. The resulting white solid mass was removed from the reactor and grounded in an analytical mill (IKA M20 basic analytical mill, IKA®-Werke GmbH & Co. KG, Staufen, Germany). The powder was washed by stirring it for 4 h with deionized water at 55 °C and left overnight at room temperature. After this, the mixture was filtered, washed with EtOH, and dried at 60 °C for 8 h in a vacuum oven (VaciotermT). The copolyamides were synthesized by following the same melt-polycondensation methodology from different mixtures of nylon 1010 and 410 salts. For each copolyamide, a total mass of 30 g of "nylon salt" was introduced into the glass reactor, where the corresponding amount of nylon 1010 salt was mixed with 12.5 mol% (10 wt%), 25 mol% (20.5 wt%), and 37.5 mol% (31.7 wt%) of nylon 410 salt to respectively produce the here so-called PA1010/410-13, PA1010/410-25, and PA1010/410-37 samples. In all cases, an excess of 10 mol% of putrescine was used to prevent stoichiometric imbalance due to diamine evaporation at the polymerization temperature.

2.3. Nuclear magnetic resonance spectroscopy

Proton nuclear magnetic resonance (^{1}H-NMR) and Carbon-13 Nuclear Magnetic Resonance (^{13}C-NMR) were used to quantify the composition and determine the microstructure of the copolyamides. ^{1}H NMR and ^{13}C NMR spectra were recorded in a Bruker AMX-300 and a Bruker Neo500 spectrometer, respectively at 25 °C, operating at 300.1 and 126.7 MHz. Samples of the "nylon salts" and copolyamides were dissolved at 30–40 mg ml^{-1} concentrations in TFE/$CDCl_3$ 4 : 1 vol/vol solvent mixtures, using tetramethyl silane (TMS) as internal reference. TFE is a polar solvent and exhibits strong hydrogen bonding properties, enabling it to dissolve substances that serve as hydrogen-bond acceptors, such as amides and ethers, and the resultant mixture gives signals with good resolution.[21] ^{1}H NMR spectra were recorded in a Bruker AMX-300 spectrometer at 25 °C. 128 (^{1}H-NMR) and 8192 (^{13}C-NMR) scans were recorded with 32K and 64K data points, respectively with delay times of 2 s. Spectra were processed with the Bruker 1D WIN NMR computer software.

2.4. Viscosity determination

Polyamide solutions were prepared in concentrated sulfuric acid (96%, Vidrafroc S.A., Barcelona, Spain) according to the ISO 307:2007 standard to determine the viscosity number (VN). To this end, dried polymer powder samples were dissolved in glass vials at 25 °C using magnetic stirring for 12 h for a complete sample solution. Flow-time measurements were obtained with a Type II Ubbelohde viscometer (Vidrafroc S.A.) in a 25 °C controlled water bath for each solution and sulfuric acid as blank. The VN (mL g^{-1}) values were determined following eqn (1):

$$\mathrm{VN} = \left[\left(\frac{\eta}{\eta_0}\right) - 1\right] \times \frac{1}{C} \quad (1)$$

where η (N m^{-2} s^{-1}) corresponds to the viscosity of the polymer solution in sulfuric acid, η_0 (N m^{-2} s^{-1}) is the viscosity of the sulfuric acid, η/η_0 is the relative viscosity of the polymer solution, and C (0.005 g mL^{-1}) is the concentration of the polymer solution. Molecular weight (M_W) was estimated from the Mark–Houwink–Sakurada expression, shown in eqn (2):

$$\eta = K \times {M_W}^{\alpha} \quad (2)$$

where η (cm^3 g^{-1}) is the Staudinger index or intrinsic viscosity, whereas K and α are the coefficient and molecular parameters, which describe the hydrodynamic interaction between the solvent and the macromolecules. The M_W values of PA1010 and the different PA1010/410 samples were estimated using

 This journal is © The Royal Society of Chemistry 2025

Open Access Article. Published on 15 1447. Downloaded on 18/07/47 09:14:27 .
This article is licensed under a Creative Commons Attribution 3.0 Unported Licence.

the experimental data previously reported for polyamide 6 (PA6) and polyamide 12 (PA12).[22]

2.5. Gel permeation chromatography

The weight-average molecular weight (M_W), number-average molecular weight (M_n), and dispersity ($Đ$) were determined by gel permeation chromatography (GPC) using a Waters GPC instrument (Model 410, Foster City, CA, USA) equipped with refractive index (RI) and ultraviolet (UV) detectors. Between 2–3 mg of bio-based polyamide were dissolved in 1 mL of HFIP and filtrated with a 0.22-μm polytetrafluoroethylene (PTFE) filter. Thus, 100 μl of this solution was injected to the system and eluted with HFIP at a flow-rate of 0.5 mL min^{-1}. HR5E and HR2 Waters linear Styragel columns (7.8 mm × 300 mm, pore 10^3–10^4 Å) packed with cross-linked polystyrene (PS) and protected with a precolumn were used. Poly(methyl methacrylate) (PMMA) standards with narrow M_W distributions were employed to generate the calibration curve.

2.6. Thermo-compression

The resultant polyamide powders were conditioned in desiccator cabinets at 25 °C and 0% relative humidity (%RH, P_2O_5) for 7 days before their processing. The bio-based polyamide films were obtained by thermo-compression in a hot-plate press (Model LP20, Labtech Engineering, Thailand). To produce films of approximately 150 μm, 2.5 g of polyamide powder was placed between PTFE sheets and subjected to a pre-heating for 2 min at 210 °C, followed by compression at 210 °C for 1 min at 20 bar and at 80 bar for 4 min.

2.7. X-ray diffraction analysis

Wide-angle X-ray diffraction (WAXD) experiments were performed at room temperature in the bio-based polyamide films using a Bruker AXS/D8 Advance diffractometer (Karlsruhe, Germany). The samples were scanned in reflection mode using incident CuK_α radiation (λ = 1.542 Å), while the generator was set at 40 kV and 40 mA. The data were collected over the (2θ) range of 5–50° and a step size of 0.04° min^{-1}. The 2D data were background-corrected and transformed into 1D profiles *via* integration using Match!2 software (Crystal Impact, Bonn, Germany). The degree of crystallinity was obtained by calculating the intensity of the diffraction peak of the polyamide crystal region and the amorphous region. The areas of crystal region and the amorphous region were obtained by peak fitting using Origin software (OriginLab Corporation, Northampton, MA, USA). The crystallinity degree (X_C, %) was calculated by using the following equation:

$$X_C = \frac{A_C}{A_C + A_A} \times 100 \quad (3)$$

where A_C is the crystalline area and A_A is the amorphous area.

2.8. Fourier transform infrared spectroscopy

Variable-temperature Fourier transform infrared (FTIR) spectroscopy was performed on a Thermo Nexus FTIR instrument fitted with a mercury cadmium telluride (MCT) detector from Thermo Fisher Scientific Inc. (Wilmington, DE, USA), coupled to a variable-temperature single reflection diamond ATR sampling accessory of Specac Ltd (Orpington, UK). Spectra were collected between 4000 and 700 cm^{-1} by averaging 64 scans at a resolution of 4 cm^{-1}. The film samples were clamped directly onto the ATR crystal using a calibrated torque wrench from Specac Ltd, (Orpington, UK) set at 80 cNm, which applies a load of 350 N *via* the sample accessory anvil. FTIR spectra were collected at 25, 50, 75, and 100 °C then at 10 °C intervals up to 230 °C. Room temperature FTIR was performed on a Thermo Nicolet iS50 FTIR Spectrometer fitted with a deuterated triglycine sulfate (DTGS) detector (Wilmington, DE, USA) using the integrated single reflection diamond ATR sampling accessory. Spectra were collected between 4000 and 400 cm^{-1} by averaging 64 scans at a resolution of 4 cm^{-1}. Peak fitting of spectral profiles was performed using Fityk version 1.3.1, selecting Lorentzian line shapes and a Levenberg–Marquart fitting function.[23] Then, seven peaks were fitted in the 800–500 cm^{-1} region, with both the peak centers and linewidth permitted freedom to be optimized. The spectrum of the homopolymer was fitted first, followed systematically by the spectra for the copolymers in increasing nylon 410-unit content order. The optimized result from the previous fitting was used as the starting point for the subsequent fits.

2.9. Thermal analysis

Thermogravimetric analysis. Thermal stability was evaluated by thermogravimetric analysis (TGA) in a TGA 1 STARe System analyzer from Mettler-Toledo, Inc. (Greifensee, Switzerland). In the case of the "nylon salts", the procedure consisted of a heating ramp at 3.3 °C min^{-1} from 25 to 230 °C for the nylon 1010 salt and from 25 to 250 °C for the nylon 410 salt, followed by an isotherm at the final temperature for 3 h to simulate thermal conditions faced during polymerization. For the bio-based polyamide films, the heating program was set from 25 to 800 °C at a heating rate of 20 °C min^{-1}. All samples were analyzed with a constant N_2 flow-rate of 10 mL min^{-1} to achieve an inert atmosphere using approximately 3 mg. The TGA and first derivative thermogravimetric analysis (DTGA) curves were analyzed using a STARe Evaluation Software (Mettler-Toledo, Inc.) to obtain the temperature at 5% weight loss ($T_{5\%}$), which corresponds to the onset degradation temperature, and the degradation temperature (T_{deg}) derived from the peak value of the first derivative.

Differential scanning calorimetry. Differential scanning calorimetry (DSC) was carried out to obtain thermal transitions using a DSC 1 STARe System model from Mettler-Toledo, Inc. Around 5 mg of "nylon salt" powder or bio-based polyamide film were placed in hermetic aluminum sealed pans of 40 μL that were calibrated previously using indium standard. A dry reducing atmosphere was used to perform the analysis, using N_2 flowing at 40 mL min^{-1}. The samples were subjected to a three-step program at 10 °C min^{-1} that consisted of a first heating scan from − 40 to 260 °C, followed by a cooling scan to −40 °C and a second heating scan to 260 °C. T_g, T_m, and normalized enthalpy of melting (ΔH_m) were

Open Access Article. Published on 15 1447. Downloaded on 18/07/47 09:14:27 .
This article is licensed under a Creative Commons Attribution 3.0 Unported Licence.

obtained from the heating scans, whereas the crystallization temperature from the melt (T_C) and normalized enthalpy of crystallization (ΔH_C) were obtained from the cooling scan.

2.10. Optical evaluation

The optical properties of the polyamide films were determined using a Minolta colorimeter (CM-5, Minolta Co., Tokyo, Japan). The reflectance of the film samples was measured from 400 to 700 nm wavelength range and the transparency of the bio-based polyamide films was determined by the Kubelka–Munk theory. The 10° Supplemental Standard Observer and the Standard D65 Illuminant were applied to determine the CIE L^*a^*b (CIELAB) coordinates, chroma (C^*_{ab}), and hue (h^*_{ab}). The color difference (ΔE^*_{ab}) was determined by application of eqn (4) using the color coordinates of the PA1010 film as the reference:

$$\Delta E^*_{ab} = \sqrt{(\Delta L^*)^2 + (\Delta a^*)^2 + (\Delta b^*)^2} \quad (4)$$

Color change was evaluated with the following assessment: unnoticeable ($\Delta E^*_{ab} < 1$), only an experienced observer can notice the difference ($\Delta E^*_{ab} \geq 1$ and < 2), an unexperienced observer notices the difference ($\Delta E^*_{ab} \geq 2$ and < 3.5), clear noticeable difference ($\Delta E^*_{ab} \geq 3.5$ and < 5), and the observer notices different colors ($\Delta E^*_{ab} \geq 5$).[24]

2.11. Tensile tests

The tensile properties of the bio-based polyamide films were obtained following the standard method ASTM D882. The samples were film-trimmed strips of 25 mm width and 100 mm long. Prior to the test, film thickness was measured in 10 random points of each sample and all of them were conditioned at 53% RH and 25 °C in a desiccator cabinet with a saturated $Mg(NO_3)_2$ solution. The strips were stretched until breaking at a rate of 12 mm min^{-1}. Force-deformation curves were obtained and transformed into stress–strain curves considering sample sizing, thickness, and deformation.

2.12. Permeability measurements

The ASTM E96-95 gravimetric method was modified to determine water vapor permeability (WVP) gravimetrically, using Payne permeability cups. The test was carried out at 25 °C and a RH gradient from 53% to 100% since it represents conditions of intermediate humidity. An analytical balance Sartorius ME36S (Fisher Scientific, Hampton, NH, USA) with an accuracy of ±0.00001 g was used to weigh the cups at intervals of 1.5 h for 24 h once the steady state was reached. The water vapor transmission rate (WVTR) was obtained from the slope of the weight loss *vs.* time. The transmission rate was corrected for permeant partial pressure to yield permeance, which was finally corrected with film thickness to obtain WVP. A similar procedure was followed to determine limonene permeability (LP), where 5 ml of D-limonene was placed instead of water inside the Payne permeability cups under the same controlled room conditions of 25 °C and 53% RH. For both measurements, cups with aluminum films were used as control samples to estimate and subtract the vapor loss through the sealing. Empty cups were used to correct the weight corresponding to the vapor uptake of the film samples during analysis. All measurements were performed in triplicate.

The ASTM Standard Method D3985-05 was applied to attain oxygen permeability (OP). Film samples of 50 cm^2 were measured using an Oxygen Permeation Analyzer (Model 8101e, Systech Illinois, Thame, UK) at 25 °C and 53% RH. Oxygen permeance was obtained from the oxygen transmission rate (OTR) corrected with the partial pressure on both film sides. Permeance was finally corrected with film thickness to obtain OP. Measurements were recorded in triplicate.

2.13. Shelf-life tests

Preparation of beef meat samples. The films were used as lids in aluminum trays in order to evaluate their performance for the shelf life of beef meat. All utensils and work surfaces were disinfected with 96% ethanol (Panreac S.A., Barcelona, Spain) before sample preparation to avoid cross-contamination. In addition, films and aluminum trays were sterilized for 1 h in ultraviolet (UV) light exposure in a laminar flow cabinet (Bio II Advance, Telstar, Terrasa, Spain). The minced beef was stored immediately after purchase in a refrigerator at 5 °C. Thus, 10 g of minced beef were placed in aluminum trays sizing 6.6 cm of diameter and 2.3 cm in height (WPAL-050-100, Quima S.L., Valencia, Spain). After this, the bio-based polyamide films were manually sealed with an extra instant adhesive glue (Pattex Cocodrile, Ferretería Moreno, Valencia, Spain). All samples were handled inside the laminar flow cabinet and stored after packaging under refrigerated conditions of 5 °C and 48% RH. These conditions were selected in accordance with previous studies that evaluated the performance of films in meat preservation.[25–27] Three samples for each treatment and time were characterized in terms of pH, weight loss, color, and microbial counts at day 0 (unpackaged meat) and after 6 and 11 days of storage under refrigerated conditions.

Physicochemical evaluation. A digital pH meter (Mettler-Toledo, Inc.) was used to measure the pH of the minced beef meat by inserting the glass electrode probe into the minced beef meat. Six measurements were taken for each packaging treatment and time. An analytical balance (ME36S, ±0.0001 g accuracy) was used to determine, in triplicate, the weight loss of the samples as a function of time. The time evolution of the CIE $L^*a^*b^*$ color coordinates, C^*_{ab}, h^*_{ab}, and ΔE^*_{ab} (eqn (4)) of the minced beef meat packaged inside the bio-based polyamide films were measured using the MINOLTA colorimeter (model CM-5). The optical values were determined using the D65/10° illuminant at six random points whereas the reflection spectrum of the samples was measured from 400 to 700 nm.

Microbial analysis. Microbiological analyses of the packaged minced beef meat were performed at different storage times: day 0 (before packaging) and after 6 and 11 days, based on the method described by Hernández-García *et al.*[27] The minced beef sample was aseptically removed from the trays using a sterile spatula in the laminar flow cabinet and placed in a sterile stomacher strainer bag (Seward Limited, West Sussex,

 This journal is © The Royal Society of Chemistry 2025

Open Access Article. Published on 15 1447. Downloaded on 18/07/47 09:14:27 .
This article is licensed under a Creative Commons Attribution 3.0 Unported Licence.

UK) with 90 mL of buffered peptone water and mixed for 3 minutes with a Masticator Paddle Blender (IUL S.A., Barcelona, Spain), to obtain a 10-fold primary dilution. Serial dilutions were then made from the homogenate, using peptone water, to determine total coliforms (TCC), lactic acid bacteria (LAB), and total viable counts (TVC) using VRB, MRS, and PCA plates, respectively. Incubation was carried out at 37 °C for 48 h for TCC and TVC and at 30 °C for 72 h for LAB. After incubation, the colonies were counted, and the results were expressed as $\log_{10}$ colony-forming units per gram of sample (log CFU per g sample).

2.14. Statistical analysis

The Statgraphics Centurion XIX software from Manugistics Corp. (Rockville, MD, USA) was used to subject tensile tests, thermal analysis, X-ray diffractograms, optical analysis, permeability measurements, and microbiological analysis of the packaged minced beef meat evaluated during storage to an analysis of variance (ANOVA). Fisher's least significant difference (LSD) procedure at the 95% confidence level was used.

3. Results

3.1. Synthesis and chemical characterization

PA1010 and different PA1010/410 were synthesized by melt polycondensation using different molar ratios of the nylon 410 and 1010 salts, which are organic substances formed by neutralization of an organic acid with organic base. These Zwitterions constitute the precursors of the bio-based polyamides and are formed by continuous hydrogen-bonded chains of $[NH_3(CH_2)_4NH_3]^{2+}$ $[OOC(CH_2)_8COO]^{2-}$ and $[NH_3(CH_2)_{10}NH_3]^{2+}$ $[OOC(CH_2)_8COO]^{2-}$, respectively.

Prior to performing the polymerization reaction, the thermal stability and characteristics of both salts were ascertained by TGA and DSC measurements and the resultant curves are included in Fig. 1. As earlier performed,[12] TGA was conducted to simulate the thermal conditions faced during polymerization. One can observe in Fig. 1a that, at these conditions, the setpoint temperature of 230 °C and 250 °C was reached after approximately 62 and 75 min for the nylon 1010 and 410 salts, respectively. Thereafter, at the given setpoint temperatures, the "nylon salt" samples showed respective mass losses of nearly 14% and 19%, respectively. Then, during the isothermal conditions, the mass progressively decreased, after 3 h reaching a value of approximately 83% and 64%, respectively. The mass loss associated to this stage is mainly related to the water released progressively during the growth of the bio-based polyamide chains. However, the absence of a plateau in the case of the nylon 410 salt suggests that thermal degradation occurs simultaneously, differing from the thermal behavior of the nylon 1010 salt. In fact, as one can observe in the TGA curves shown in Fig. 1b, both salts presented a mass loss of ~1% at 100 °C, ascribed to the evaporation of the

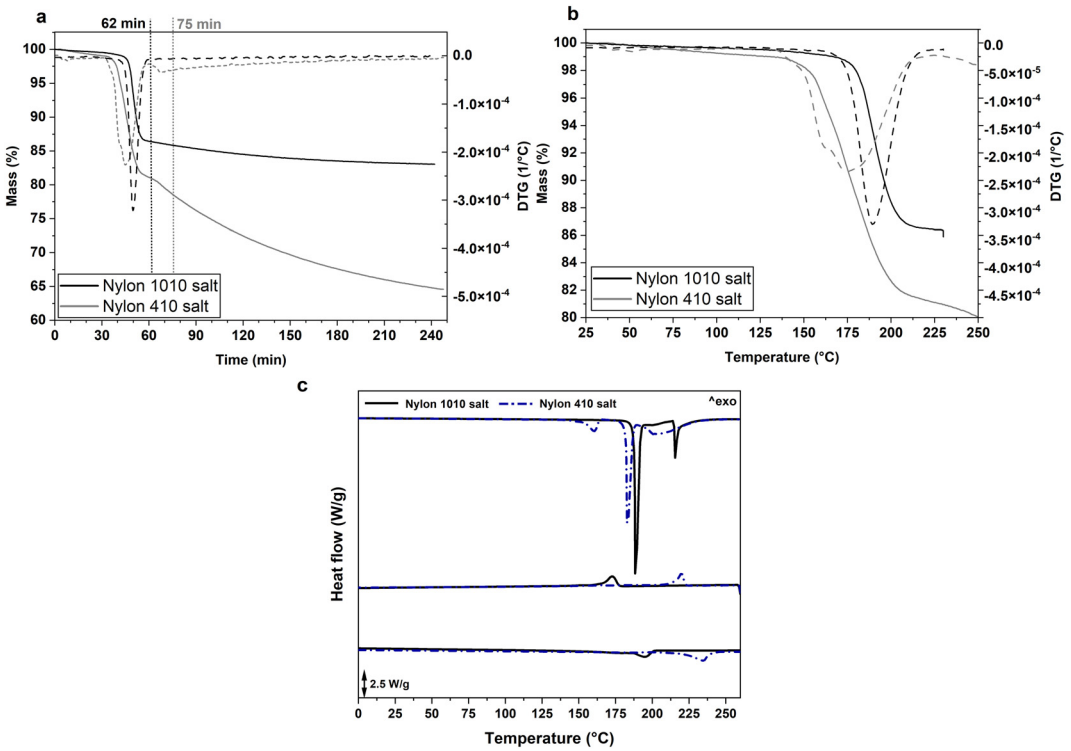

Fig. 1 Thermogravimetric analysis (TGA) and first derivative thermogravimetric analysis (DTGA) curves as a function of time (a) and temperature (b) of the nylon 1010 and 410 salts; differential scanning calorimetry (DSC) curves corresponding to, from top to bottom, first heating, cooling, and second heating of the "nylon salts" (c).

Open Access Article. Published on 15 1447. Downloaded on 18/07/47 09:14:27 .
This article is licensed under a Creative Commons Attribution 3.0 Unported Licence.

remaining solvents or sorbed water. Then, thermal degradation onset was seen to occur in the nylon 1010 and 410 salts at ~176 °C and ~150 °C, respectively, which was seen to follow by a sharp peak centered at approximately 189 °C and 179 °C. Therefore, the TGA measurements carried out on the "nylon salts" indicates that the thermal stability of the 410 units is much lower than those of 1010, which may restrict the use of high-temperature conditions during polymerization.

The thermal transitions of the salts were further studied by means of DSC, and Fig. 1c confirmed the melting and subsequent polymerization of the "nylon salts" to form the respective PA1010 and PA410 homopolyamides. In particular, during the first heating, the nylon 1010 and 410 salts melted at nearly 189 °C and 183 °C, respectively. After melting, one can further observe that both salts formed an oligomer or prepolymer that crystallized, showing T_C values of ~177 °C and ~221 °C, respectively. Finally, the resultant oligomers or low-M_W bio-based homopolyamides melted during the second heating, showing respective values of T_m of ~197 °C and ~237 °C. These results facilitated the selection of the melt polycondensation temperature and the previous thermal conditions used to analyze the "nylon salts" by TGA, that is, 230 °C for 1010 and 250 °C for 410, to ensure full melting of the salt crystals.

Fig. 2 displays the ^{1}H-NMR spectra of the "nylon salts", the precursors used in the synthesis of the copolyamides. As can be observed in Fig. 2a, signals due to the CH_2 groups of the diamine that appear at 2.98 ppm displayed peaks with equal intensity to the ones of the diacid group appearing at 2.23 ppm, indicating the effective preparation of these intermediate products. After polymerization, these two signals moved to a low and high field, respectively, ascertaining the successful synthesis of PA1010 and the different PA1010/410 copolyamides (see Fig. 2b). Signals due NH of CONH groups appeared in the low field region (6.4–6.8 ppm) and were used for the determination of the copolyamide composition. As can be observed in Table 1, the final composition was close to the feed composition, indicating that both "nylon salts" successfully reacted almost quantitatively. Signals due to the CH_2 attached to the CONH group appeared at 3.2 ppm, whereas the signal due to the CH_2 attached to the carbonyl (C═O) group was seen at 2.15 ppm. The inner CH_2 groups corresponding to the long alkylene chains appeared in the high field region at the 1.6–1.2 ppm range.

Furthermore, ^{13}C NMR was used for the study of the bio-based copolyamides microstructure. Under these melt polycondensation conditions, amidation and transamidation reactions are both expected to occur at the employed temperatures, potentially leading to a random copolyamide microstructure. In Fig. 2c, one can observe two signals splitting around 39.5 and 36.4 ppm due to the methylene carbons next to the NH and C═O groups, respectively. The peaks around 176 ppm correspond to C═O groups, whereas the peaks between 30–25 ppm are assigned to the rest carbons of the long CH_2 segment. This peak assignment agrees with previous literature observed for different nylons.[28] The splitting of the signals

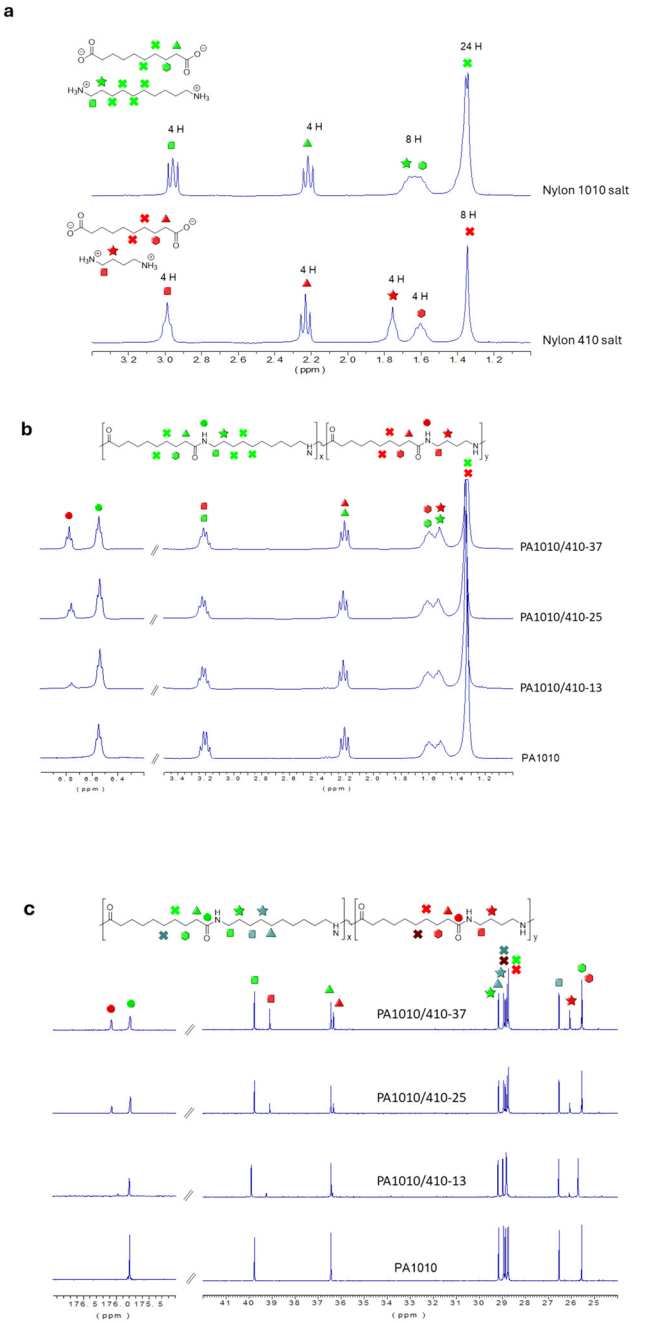

Fig. 2 Proton nuclear magnetic resonance (^{1}H-NMR) spectra with peak assignments of nylon 410 and 1010 salts (a) and polyamide 1010 (PA1010) and copolyamides 1010/410 (PA1010/410) (b). Carbon-13 Nuclear Magnetic Resonance (^{13}C-NMR) spectra with peak assignments of PA1010 and PA1010/410 (c).

corresponding to the methylene carbon attached to the C═O group of the sebacic unit was attributed to its sensitivity to the adjacent unit connected through the amide group (either butylene or decamethylene). However, no additional splitting arising from the presence of butylene or decamethylene units on the opposite side of the sebacamide unit could be observed. This prevented the determination of the sequence distribution

 This journal is © The Royal Society of Chemistry 2025

Open Access Article. Published on 15 1447. Downloaded on 18/07/47 09:14:27 .
This article is licensed under a Creative Commons Attribution 3.0 Unported Licence.

Table 1 Molar feed composition and copolyamide composition, viscosity number (VN), and weight-average and number-average molecular weight (M_W and M_n) and dispersity ($Đ$) of polyamide 1010 (PA1010) and copolyamides 1010/410 (PA1010/410)

Sample	Feed composition (1010 mol%/410 mol%)	Copolyamide composition[a] (1010 mol%/410 mol%)	VN (mL g^{-1})	M_n [b] (g mol^{-1})	M_W [b] (g mol^{-1})	$Đ$[b]
PA1010	100/0	100/0	101 ± 1	11 255	39 210	3.5
PA1010/410-13	87.5/12.5	86.8/13.2	60 ± 1	8400	17 950	2.1
PA1010/410-25	75/25	72.3/27.7	63 ± 1	13 100	19 141	1.5
PA1010/410-37	62.5/37.5	62.5/37.5	75 ± 1	14 300	23 500	1.6

[a] Determined by proton nuclear magnetic resonance (^{1}H-NMR). [b] Determined by gel permeation chromatography (GPC).

and, consequently, the microstructure of the bio-based copolyamides. In fact, no sequence-related splitting could be detected in any carbon signal, even though the spectra were processed without exponential multiplication to enhance resolution. This lack of sensitivity to variations in the local chemical environment is most likely due to the considerable length of both the diacid and the diamines employed in the synthesis of these copolyamides. Similar results were reported by Koning and coworkers,[19] who found that the ^{13}C NMR spectra of comparable copolyamides derived from sebacic acid did not provide information on the copolymer microstructure.

Table 1 also includes the VN values attained for the synthesized PA1010 and PA1010/410 with different putrescine contents. The VN of the homopolyamide was 101 ± 1 cm^3 g^{-1}, which is lower than that reported earlier for PA1010 (130 ± 5 cm^3 g^{-1}).[12] This difference can be related to the use of milder conditions during the polymerization reaction. For instance, Li *et al.*[29] reported different viscosity values for polyamide 1214 (PA1214), ranging from 84 to 126 cm^3 g^{-1} due to variations of temperature, pressure, and time. One can observe that the incorporation of the nylon 410 salt resulted in a decrease in the VN to 60 ± 1 cm^3 g^{-1} (PA1010/410 with 12.5 mol% nylon 410) and 63 ± 1 cm^3 g^{-1} (PA1010/410 with 25 mol% nylon 410). Interestingly, further increase in the nylon 410 salt to 37.5 mol% resulted in an increase in the VN value to 75 ± 1 cm^3 g^{-1} (PA1010/410 with 37.5 mol% nylon 410), suggesting superior polyamidation at higher putrescine contents. Similar results were obtained by Rwei *et al.*[20] for copolyamides of nylon 6 (PA6) with N1,N6-bis(4-aminobutyl) adipamide and succinic acid (BABA/SA), observing a reduction in the polyamidation at lower BABA/SA contents followed by an increase at higher contents.

The application of the Mark–Houwink equation, based on the parameters reported for PA6 and PA12,[22,29] resulted in M_W values in the range of 2.9–8.8 × 10^4 g mol^{-1} for the PA1010 homopolyamide and of 1.5–3.9 × 10^4 g mol^{-1} (PA1010/410 with 12.5 mol% nylon 410), 1.6–4.2 × 10^4 g mol^{-1} (PA1010/410 with 25 mol% nylon 410), 2.0–5.5 × 10^4 g mol^{-1} (PA1010/410 with 37.5 mol% nylon 410) copolyamides. The lower viscosity values and hence M_W attained in the bio-based copolyamides can be ascribed to high volatility of putrescine and lower thermal stability of the nylon 410 salt, as previously determined by TGA. In this regard, at elevated temperatures, 1,4-diaminobutane can be partially transformed into pyrrolidine, which is a potential chain stopper during polyamide chain growth, being present as a third end group in addition to carboxylic acid and amine groups.[30] The resultant values are similar to those of the fully bio-based aliphatic copolyamide 1010/1014 (PA1010/1014) synthesized by our group previously, which was 67 cm^3 g^{-1} and corresponds to a M_W in the range of 2.0–6.5 × 10^4 g mol^{-1}.[31] Similar results were also obtained by Cui *et al.*,[28] who observed that polyamide 411 (PA411) resulted in lower intrinsic viscosity and M_W values (0.51 dL g^{-1} and 8.4 × 10^3 g mol^{-1}) than other nylons due to the particularly high volatility of diaminobutane.

As can also be further seen in Table 1, GPC analysis confirmed that polyamides with moderate M_Ws were obtained. In particular, PA1010 presented a M_W value of 3.92 × 10^4 g mol^{-1}, whereas the M_W values of the copolyamide PA1010/410 grades ranged from 1.79 to 2.35 × 10^4 g mol^{-1}, being all the $Đ$ values in the 1.5–3.2 range. Although such fluctuations can significantly affect crystallization–melting behavior and physical performance of the copolyamides, the polymerization conditions were maintained to also ascertain the effect of the comonomer content on their final M_W characteristics. Moreover, the M_W variations within the copolyamide compositions were relatively low. For the homopolyamide, the resultant M_W value determined herein was similar than that of the commercial PA1010 grade for injection molding applications, that is, 3.98 × 10^4 g mol^{-1} with $Đ$ equals to 2.5.[32] The evolution of the M_W values of the copolyamides also agrees with the viscosity measurements, which are in the range but lower than the homopolyamide. Nevertheless, their M_W are still in the range of other green nylons, with values varying from ~2500 g mol^{-1} upward or from 7200 g mol^{-1} to above 1.30 × 10^4 g mol^{-1}.[28] In terms of food packaging, the here-developed bio-based copolyamides with moderate M_W can facilitate their processability and improve SIT behaviour.[28,33] In any case, further optimization of the polymerization process should be considered to achieve smaller variations in both the M_W and M_W distribution among the bio-based copolyamide formulations.

3.2. Crystallinity and structure

Room-temperature WAXD measurements were performed to determine the crystalline percentage, that is, X_C, and the structure of the PA1010/410 copolyamides. The resultant diffractograms are gathered in Fig. 3. PA1010 showed three main diffr-

Open Access Article. Published on 15 1447. Downloaded on 18/07/47 09:14:27 .
This article is licensed under a Creative Commons Attribution 3.0 Unported Licence.

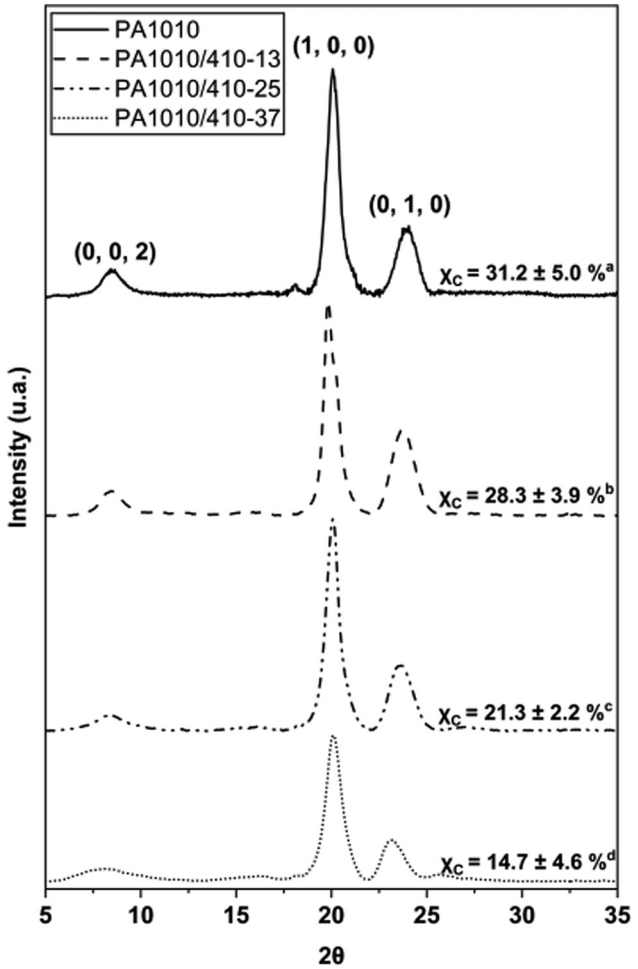

Fig. 3 X-ray diffractograms with peak assignments of polyamide 1010 (PA1010) and copolyamides 1010/410 (PA1010/410) with different contents of putrescine. Different superscripts ($^{a-d}$) in the percentage of crystallinity (χ_c) values indicate significant differences among the samples ($p < 0.05$).

action peaks located at 2θ = 8.32°, 20.30°, and 24.47°, corresponding to the d spacing of 1.0618 nm, 0.4371 nm, and 0.3635 nm, respectively.[34] These three diffraction peaks have been correspondingly ascribed to the (002), (100), and (010/110) planes from the monoclinic triclinic α-crystal form of PA1010.[35] Although for all synthesized bio-based polyamides the α-crystalline phase dominated the structure, the characteristic diffraction peaks of the α-crystalline phase of PA1010 broadened and their intensity decreased with the partial substitution of diaminodecane by putrescine. Moreover, the ratio of (100) *vs.* (010/110) peak intensities decreased due to reduction of repeating unit length whereas all peaks shifted slightly towards lower 2θ values, indicating an increase in inter-chain- and inter-sheet distance.[19] Therefore, WAXD experiments suggest that increasing the 410-unit content enlarges the 010/110 crystal plane spacing.

Thus, the incorporation of putrescine disrupted PA1010 crystal formation and, as a result of this, the X_C values progressively decreased. Whereas the PA1010 homopolyamide showed a crystallinity of 31.2%, the different bio-based copolyamides exhibited crystallinity values of 28.3%, 21.3%, and 14.7% for PA1010/410-13, PA1010/410-25, and PA1010/410-37, respectively. These results agree with previous literature values since crystallinities of these polyamides habitually range at 40–20%.[36] In addition, crystal formation tends to be favored by hydrogen-bonding in an overall less-efficient way than crystallization induced by van der Waals interaction, that is, the driving force in long-chain polyamides.[37] Therefore, the crystallizability was weakened by the incorporation of nylon-410 segments in PA1010.[19,36,37]

Variable-temperature FTIR was used to obtain more concrete information about the changes in molecular conformations and H-bonds during continuous heating. Fig. 4 shows 3D plots with the FTIR spectra as a function temperature of the PA1010 (Fig. 4a) and PA1010/410 samples (Fig. 4b–d). The strongest peaks of the PA1010 were found ~3300 cm^{-1}, which is attributable to the hydrogen-bonded N–H stretching vibration, and the coupled bands at 2857 and 2952 cm^{-1} due to the symmetric and antisymmetric stretching vibration of CH_2.[38] The other characteristic peaks of the amide groups are listed as follows: ~1632 cm^{-1} (amide I, C═O stretching vibration), ~1535 cm^{-1} (amide II, C–N stretching, and CO–N–H bending vibration), ~1460 cm^{-1} (amide III, C–N stretching, and C–H in-of-plane bending vibration), 1262 cm^{-1} (amide IV, C–CO stretching vibration), 720 cm^{-1} (CH_2 wagging), and 686 cm^{-1} (amide V, N–H out-of-plane bending vibration).[39] These data confirm the anticipated chemical structure of these copolyamides.

In all instances, as a function of heating, one can observe that the hydrogen bonding within the samples decreases with increased temperature. This is evidenced by systematic shifts to higher wavenumber of bands associated with ν(NH) and ν(C═O), seen ~3300 and 1635 cm^{-1}, respectively. For the homopolyamide, the ν(NH) started ~3303 cm^{-1} at room temperature and shifted to ~3316 cm^{-1} at 210 °C. Whilst the ν(C═O) was ~1632 cm^{-1} at room temperature and ~1637 cm^{-1} at 210 °C. In both cases, the shifts in peak position were accompanied by dramatic decreases in band intensity. Similar observations are made for the copolymer systems with overall shifts of ~10 cm^{-1} measured for ν(NH) and ~5 cm^{-1} for ν(C═O) between spectra collected room temperature and 210 °C. In the particular case of PA1010/410-37, these shifts were even greater as the temperature exceeds the melting point, with shifts of ~22 cm^{-1} for the ν(NH) and ~15 cm^{-1} for ν(C═O) noted in the spectrum collected at 210 °C.

The effect of the nylon 410-unit content on the hydrogen bonding and crystallization behavior of the bio-based polyamides was further elucidated by FTIR analysis and shown in Fig. 5. Thus, Fig. 5a shows a comparison of the FTIR spectra collected at room temperature for PA1010 homopolyamide and all the PA1010/410 copolyamides. In Fig. 5b one can observe that the band positions of the stretching vibrations of N–H, which are influenced by the hydrogen bonding within the PA1010/410 copolyamides, slightly shifted to lower wavenum-

 This journal is © The Royal Society of Chemistry 2025

Open Access Article. Published on 15 1447. Downloaded on 18/07/47 09:14:27 .
This article is licensed under a Creative Commons Attribution 3.0 Unported Licence.

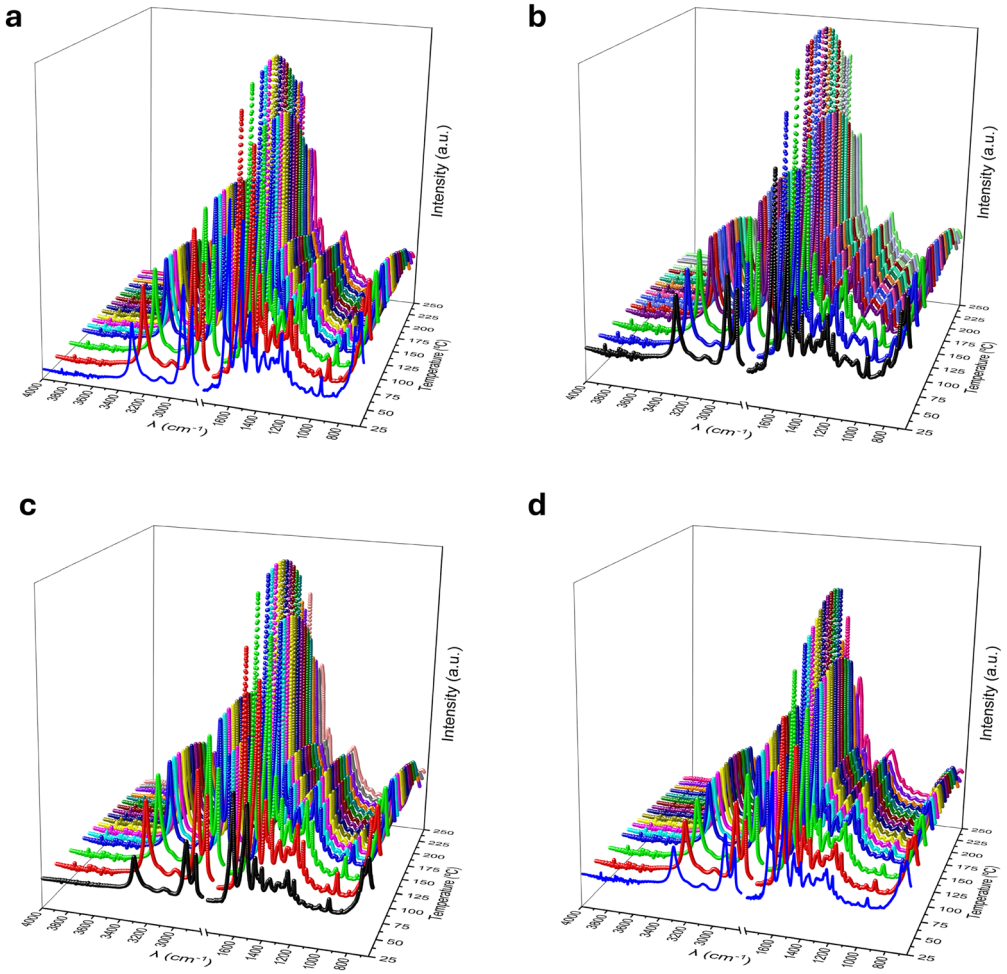

Fig. 4 Fourier transform infrared spectroscopy (FTIR) spectra taken across temperature of the homopolyamide 1010 (PA1010) (a) and copolyamides 1010/410: PA1010/410 with 12.5 mol% nylon 410 (b), PA1010/410 with 25 mol% nylon 410 (c) and PA1010/410 with 37.5 mol% nylon 410 (d).

ber with an increase in the proportion of nylon 410 segments. These shifts are indicative of an increase in the overall hydrogen bonding as the nylon 410-unit content in the copolyamide is increased. The expectation would be that this phenomenon would be accompanied by a complementary shift to lower wavenumber of the ν(C═O) band position, which is also known to change with H-bonding. Intriguingly, there was no obvious change in the peak position of the amide I, however, there were noted increases in intensity with increased nylon 410-unit content relative to the C–H scissoring and bending modes between 1480 cm^{-1} and 1400 cm^{-1} and these changes are quantified in Fig. 5c. This, one assumes, is due to both the increase in the number of carbonyl groups relative to the number of methylene repeat units as the composition changes and the increase in hydrogen bonding strength between amide segments.[40] One considers that the observed peak position of the amide I is therefore a competing balance between the intrinsic peak center of the nylon 1010 and 410 amide segments and changes in the hydrogen bonding within the copolyamides. Also, of interest in this region of the spectrum is the relative peak intensity of the amide I ν(C═O) to the amide II δ(NH). In the case of the PA1010 homopolyamide, the amide I band presented a greater intensity than the amide II band. Nevertheless, with the addition and subsequent increase of nylon 410-unit content, the amide II band was stronger than the amide counterpart for all compositions of copolymer.

Additional information relating to the crystallization within these bio-based copolyamides can be elucidated by the change in the band intensities in the 780–500 cm^{-1} region, shown in Fig. 5d. This region of the spectrum contains the amide V (N–H out-of-plane mode) ~690 cm^{-1} and the amide VI (C═O out-of-plane mode) ~580 cm^{-1}, typical of the planar zig-zag structure of the α-form of nylon 1010.[41] The amide V band was seen to decrease in intensity and broaden (*cf.* FWHM of 23.5 cm^{-1} for PA1010 *versus* 26.5 cm^{-1} for PA1010/410-37) with increased nylon 410-unit content. This band intensity reduction further confirms the above-described reduction in crystallinity with increased nylon 410-unit content. Similarly, the amide VI band was also seen to decrease in intensity and broaden as a function of increased PA410-unit content (*cf.* FWHM of 17.1 cm^{-1} for PA1010 *versus* 20.4 cm^{-1} for PA1010/410-37). Using the intensity of the isolated amide VI band, which is free of inter-

Open Access Article. Published on 15 1447. Downloaded on 18/07/47 09:14:27 .
This article is licensed under a Creative Commons Attribution 3.0 Unported Licence.

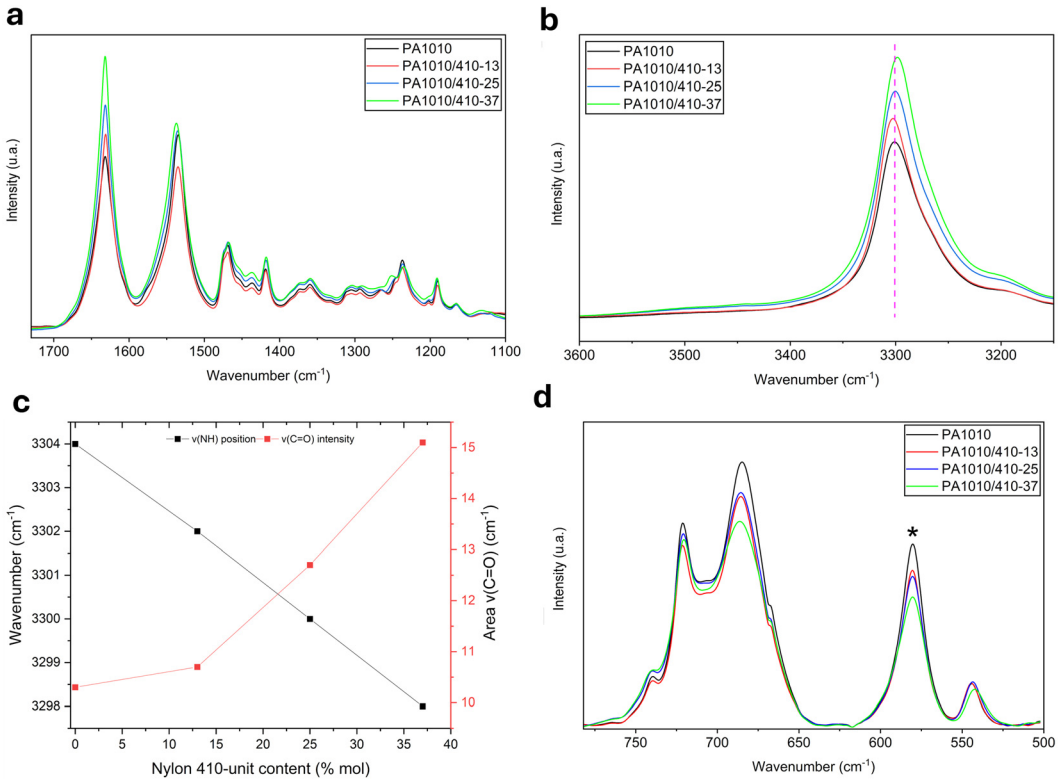

Fig. 5 (a) Fingerprint region for polyamide 1010 (PA1010) and copolyamides 1010/410 (PA1010/410); (b) N–H stretch in the 3450–3250 cm^{-1} region; (c) N–H stretch shift and C═O intensity with increasing nylon 410-unit content; (d) amide V and VI in the 800–500 cm^{-1} region, where * denotes band used to calculate crystallinity.

ference or contribution of other surrounding bands, and the measured crystallinity of the PA1010 sample taken as reference, one can calculate the crystallinity of the copolyamides. To this end, the bands in the FTIR spectra between 780–500 cm^{-1} were deconvoluted (see Fig. 6). Thus, crystallinity of the copolyamides were calculated as 27.0%, 25.9%, and 22.1% for PA1010/410-13, PA1010/410-25, and PA1010/410-37, respectively. These values are comparable to those generated previously from the WAXD data.

3.3. Physical characterization

The PA1010 and PA1010/410 films were also subjected to thermal analysis to ascertain the effect of the nylon 410 content on both the thermal stability and transitions of the bio-based polyamides. Fig. 7 gathers the TGA curves (Fig. 7a) and their respective DTGA curves (Fig. 7b), whereas Table 2 summarizes the main thermal parameters obtained from these curves. All the examined bio-based polyamide samples showed two decomposition stages, indicating a two-step mechanism in the decomposition process. Thermal degradation of PA1010 is based on a β-C–H transfer reaction mechanism that produces ketoamides, as the primary decomposition products, which thereafter decompose at higher temperature.[15] The PA1010 sample was stable up to approximately 400 °C, showing a T_{deg} of 475 °C, which agrees with our previous studies.[12,15] One can further observe that the introduction of low nylon 410 contents (12.5 mol%) did not significantly ($p > 0.05$) alter the thermal stability of the bio-based polyamide. However, higher comonomer contents (25 and 37.5 mol%) increased the onset of degradation, measured as $T_{5\%}$, by approximately 20 °C. In this regard, Rwei *et al.*[20] reported a slight decrease in T_{deg} with the introduction of increasing weight percentages of nylon units with longer alkyl segments, ascribed to the relatively low stability of aliphatic CH_2 groups at high temperature. In any case, the high thermal stability of PA1010/410 makes it an ideal candidate for most food packaging applications and nearly unlimited industrial processing conditions of plastics.

As can be observed in the DSC curves shown in Fig. 8, all the bio-based polyamides presented different thermal transitions during heating (Fig. 8a) and cooling (Fig. 8b) that were affected by the nylon 410 content. The second-order transition seen in the 40–60 °C range corresponds to the T_g of the polyamides.[32] Interestingly, the putrescine content slightly reduced the T_g values of PA1010/410, which varied from approximately 57 °C, for the homopolyamide, down to 40 °C at the highest PA410 content. Although the glass transition region of PA1010 was difficult to elucidate,[15] this became more noticeable in the case of the copolyamide grades due to their reduction in crystallinity. Furthermore, the thermographs taken during cooling revealed that both the T_C and ΔH_C values were also significantly reduced with the increase in putrescine. In particular,

 This journal is © The Royal Society of Chemistry 2025

Open Access Article. Published on 15 1447. Downloaded on 18/07/47 09:14:27 .
This article is licensed under a Creative Commons Attribution 3.0 Unported Licence.

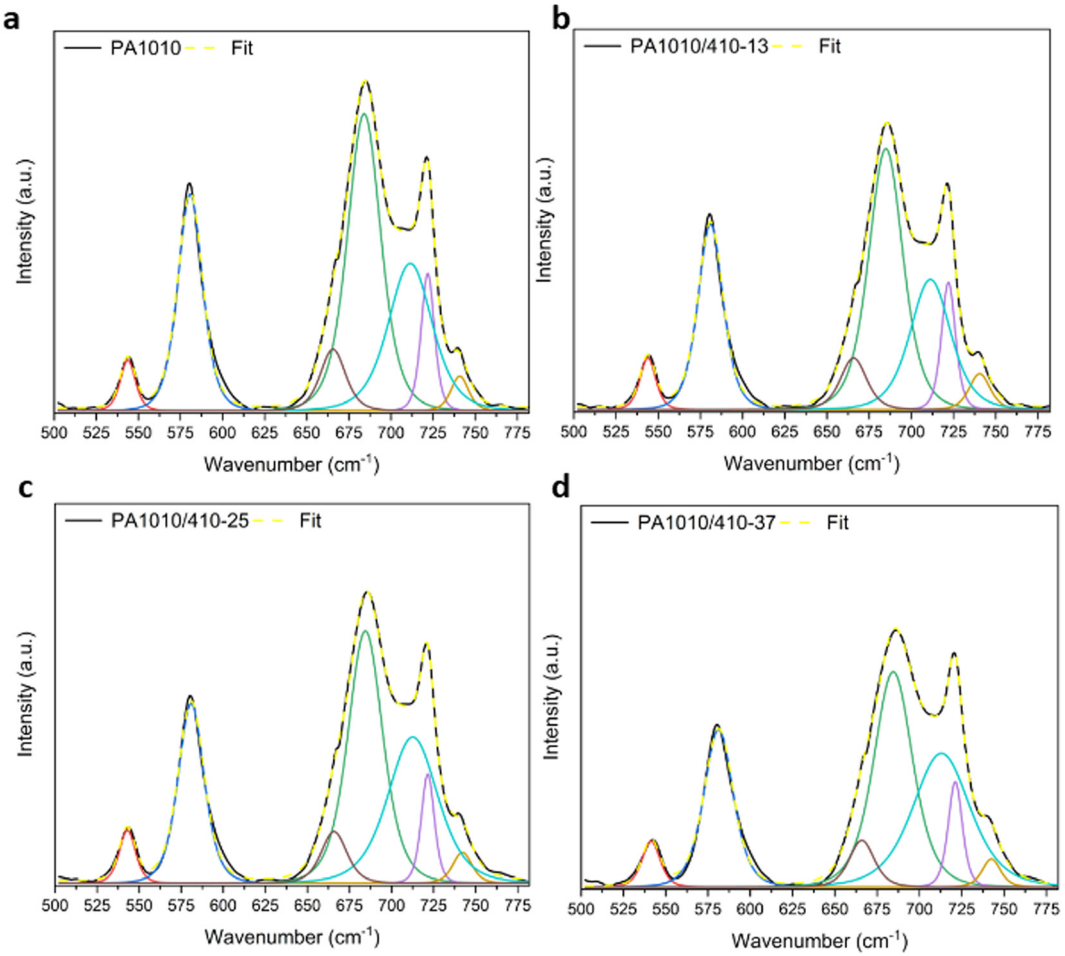

Fig. 6 Fourier transform infrared spectroscopy (FTIR) spectra deconvoluted data for homopolyamide 1010 (PA1010) (a) and copolyamides 1010/410 with 12.5 mol% nylon 410 (PA1010/410-13) (b), 25 mol% nylon 410 (PA1010/410-25) (c) and 37.5 mol% nylon 410 (PA1010/410-37) (d).

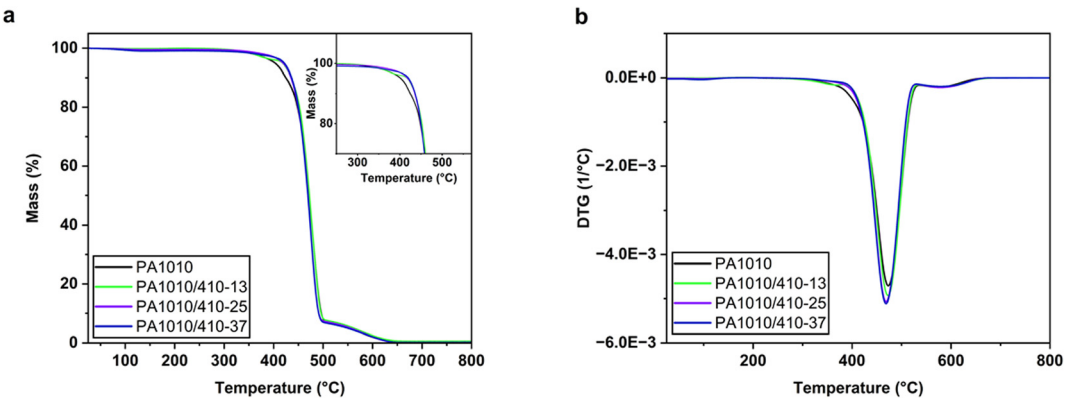

Fig. 7 (a) Thermogravimetric analysis (TGA) and (b) derivative thermogravimetric analysis (DTGA) of polyamide 1010 (PA1010) and copolyamides 1010/410 (PA1010/410) films.

T_C progressively reduced from approximately 178.5 °C, for PA1010, up to nearly 148 °C. Similarly, the values of T_m, determined in the heating thermograms, significantly reduced with the increasing content of nylon 410. Therefore, T_m decreased down to nearly 179 °C, from approximately 201 °C for PA1010.[39] In terms of ΔH_m, one can observe that the PA1010/410 presented significantly lower ($p > 0.05$) values than PA1010, further confirming the above-described reduction in

Open Access Article. Published on 15 1447. Downloaded on 18/07/47 09:14:27 .
This article is licensed under a Creative Commons Attribution 3.0 Unported Licence.

Table 2 Thermal properties of polyamide 1010 (PA1010) and copolyamides 1010/410 (PA1010/410) films in terms of glass transition temperature (T_g), crystallization temperature (T_C), enthalpy of crystallization (ΔH_C), cold crystallization temperature (T_{CC}), enthaply of cold crystallization (ΔH_{CC}), melting temperature (T_m), enthalpy of melting (ΔH_m), temperature at 5% weight loss ($T_{5\%}$), degradation temperature (T_{deg}), mass loss at T_{deg}, and remaining mass at 800 °C

	DSC						TGA			
Sample	T_g (°C)	T_C (°C)	ΔH_C (J g^{-1})	T_{CC} (°C)	ΔH_{CC} (J g^{-1})	T_m (°C)	ΔH_m (J g^{-1})	$T_{5\%}$	T_{deg}	Mass loss at T_{deg} (%)	Remaining mass (%)
PA1010	57.1 ± 2.2^a	178.5 ± 0.4^a	85.6 ± 0.6^a	182.6 ± 0.3^a	5.5 ± 0.2^a	200.9 ± 0.9^a	−80.8 ± 2.4^a	401.5 ± 0.7^a	475.0 ± 0.0^a	48.3 ± 0.0^a	0.4 ± 0.1^a
PA1010/410-13	49.9 ± 2.3^b	169.8 ± 0.5^b	70.5 ± 0.8^b	175.2 ± 0.2^b	5.9 ± 1.3^a	194.2 ± 1.7^b	−60.9 ± 2.8^b	401.5 ± 23.3^a	471.5 ± 0.7^{a,b}	49.8 ± 1.2^{a,b}	0.5 ± 0.1^a
PA1010/410-25	43.9 ± 1.8^c	155.7 ± 0.4^c	68.9 ± 0.9^c	159.6 ± 0.5^c	3.3 ± 0.5^a	181.8 ± 1.3^c	−59.7 ± 3.2^c	423.5 ± 7.8^a	470.5 ± 2.1^{a,b}	51.2 ± 0.1^b	0.3 ± 0.2^a
PA1010/410-37	39.7 ± 1.9^c	147.9 ± 1.1^d	61.2 ± 0.5^d	154.0 ± 0.3^c	1.1 ± 0.1^b	179.1 ± 1.2^c	−46.5 ± 3.1^b	421.5 ± 0.7^a	469.5 ± 2.4^b	50.9 ± 0.7^b	0.3 ± 0.1^a

Different superscript letters ($^{a-d}$) indicate significant differences among formulations ($p < 0.05$).

crystallinity in the copolyamides. It is also worth noting that, even though the polyamides cold crystallized prior to melting, all displayed a single melting peak during both heating scans, further supporting the presence of a single crystalline form, as previously described during the crystallinity assessment. The thermal properties of PA1010/410 with nylon 410 contents of 25 and 37.5 mol% are similar to those of medium- or long-chain PA12 (~179 °C)[42] and slightly higher than those of isotactic polypropylene (PP) (~161 °C).[43] This makes it easily processable and feasible to seal in most multilayer structures used in food packaging.[5]

From the above, it was seen that the bio-based copolyamides crystallized in the entire composition range studied herein. However, the crystallization/melting of random copolymers is a complex function of the chemical structure of the repeating units involved, molar ratio of comonomers, and M_W. Indeed, the thermal transitions determined by non-isothermal DSC experiments indicate that these copolyamides show isodimorphic behavior with a moderate amount of comonomer exclusion.[44] In this regard, one can observe in Fig. 9 that the bio-based polyamides presented first-order thermal transition (T_C and T_m) values with non-linear dependence on molar composition: PA1010 (~178.5 and 201 °C), PA1010/410-13 (~169 and 194 °C), PA1010/410-25 (~156 and 182 °C), PA1010/410-37 (~148 and 179 °C), and PA410 (~226 and 250 °C).[45] Therefore, the comonomers crystallized in the same crystal lattice, but with partial inclusion of nylon 410-units in the unit cell of nylon 1010. From the plots, it can be inferred that both 410- and 1010-units were hosted in the PA1010/410 crystals, but these were characterized by a PA1010-rich crystalline phase with a "pseudo-eutectic" region in the 25–37 mol% range. At this molar composition, the melting point of the PA1010 phase was depressed by the presence of nylon 410-units down to a temperature of approximately 180 °C.

Variable temperature FTIR studies reported above were also used to provide complementary information relating copolymer composition to structural changes as a function of temperature. Fig. 10 gathers the normalized band area at 1190 cm^{-1}, which is ascribed to CH_2 wagging. One can observe the sharp decrease in this band area in the 200–180 °C range due to polyamide melting. Collecting the FTIR spectra of green nylons as a function of temperature also resulted in changes to a number of bands. Specifically, one observes the major changes in the shift to higher wavenumber of 3304 cm^{-1} at room temperature to 3317 cm^{-1} in the melt and a reduction in intensity in the amide II peak. In addition, a new band ~3450 cm^{-1} appeared in the melt that we can ascribe to 'free' ν(N–H).[46] These were accompanied by complementary shifts to higher wavenumber, from 1631 cm^{-1} at room temperature to 1642 cm^{-1} in the melt, with a significant broadening. This confirms the hydrogen bond strength reduction in the copolyamides and further supports the development of an isodimorphic random copolyamide formed by a PA1010-rich crystalline phase with partial inclusion of 410-units. Furthermore, this is also in agreement with above-reported WAXS experi-

This journal is © The Royal Society of Chemistry 2025

Open Access Article. Published on 15 1447. Downloaded on 18/07/47 09:14:27 .
This article is licensed under a Creative Commons Attribution 3.0 Unported Licence.

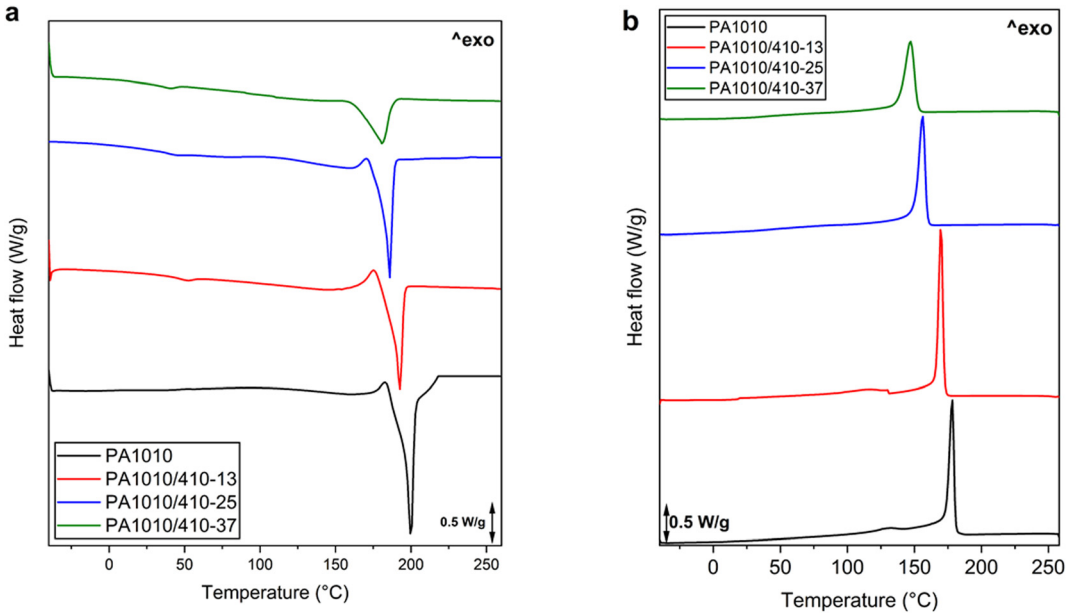

Fig. 8 Differential scanning calorimetry (DSC) curves corresponding to (a) first heating and (b) cooling of polyamide 1010 (PA1010) and copolyamides 1010/410 (PA1010/410) films.

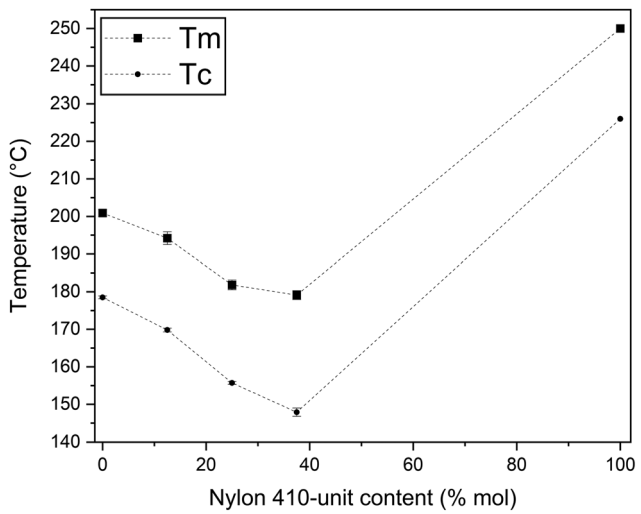

Fig. 9 Evolution of the crystallization (T_C) and melting temperature (T_m) as a function of the nylon-410 unit content in copolyamides 1010/410 (PA1010/410).

ments, showing the 010/110 crystal plane spacing enlargement when the nylon 410-unit content was increased.

Film transparency and color are also important factors in food packaging designs. In Fig. 11 the optical properties of the bio-based polyamide films were analyzed to ascertain the effect of putrescine, whereas Table 3 summarizes the color coordinates in terms of L^*, C^*_{ab}, and h^*_{ab} as well as the total color difference, expressed as ΔE^*, concerning the homopolyamide PA1010 film. Fig. 11a represents the spectral distribution curve of the percentage of T_i of the PA1010 and PA1010/410 films as a function of wavelength (λ). All the bio-based polyamide films showed relatively high values of T_i, ranging from 70% to 87%, indicating that the samples highly transmitted light. This transparency is close to that of polyethylene terephthalate (PET) films and in the range of other biopolymers of interest in food packaging, such as poly(3-hydroxybutyrate-*co*-3-hydroxyvalerate) (PHBV).[47] However, the copolyamide films exhibited lower transparency than the homopolyamide PA1010 film, presenting lower values of T_i at the lowest wavelength. This reduction in T_i, particularly relevant in the near-ultraviolet (UV) spectral region close to 400 nm, can be explained mainly by the development of a yellow color, which was particularly noticeable in the PA1010/410 with 25 mol% of nylon 410 salt (see Fig. 11b). Yellowing in polyamides has been ascribed to the formation of photo-unstable by-products with color-conjugated imide groups, which is attributed to the presence of amine groups with a lone pair of electrons[48] or thermo-oxidation reaction of unsubstituted or *N*-substituted aliphatic polyamides, such as crotonized aldehydic groups ($(-CH{=}CH)_{2or3}CHO$).[49] Furthermore, the lignin residual impurities produced in the biological fermentation to obtain putrescine production can be easily oxidized and turn into a chromophore that further deepens the yellow color.[50] Thus, the "see-through" capability was reduced in the copolyamides. However, this low-light-transmission capacity could promote the protection against light-induced oxidative processes of certain foods, such as oil or meat.[51] In terms of optical properties, the copolyamide PA1010/410 film samples showed lower brightness than the PA1010 film, measured as L^*, in the 81–85 range. In relation to the a^* and b^* color coordinates, the copolyamide films were slightly green and pale yellow, leading values of the hue or tone (h^*_{ab}) in the range of 92–104 and a

Open Access Article. Published on 15 1447. Downloaded on 18/07/47 09:14:27 .
This article is licensed under a Creative Commons Attribution 3.0 Unported Licence.

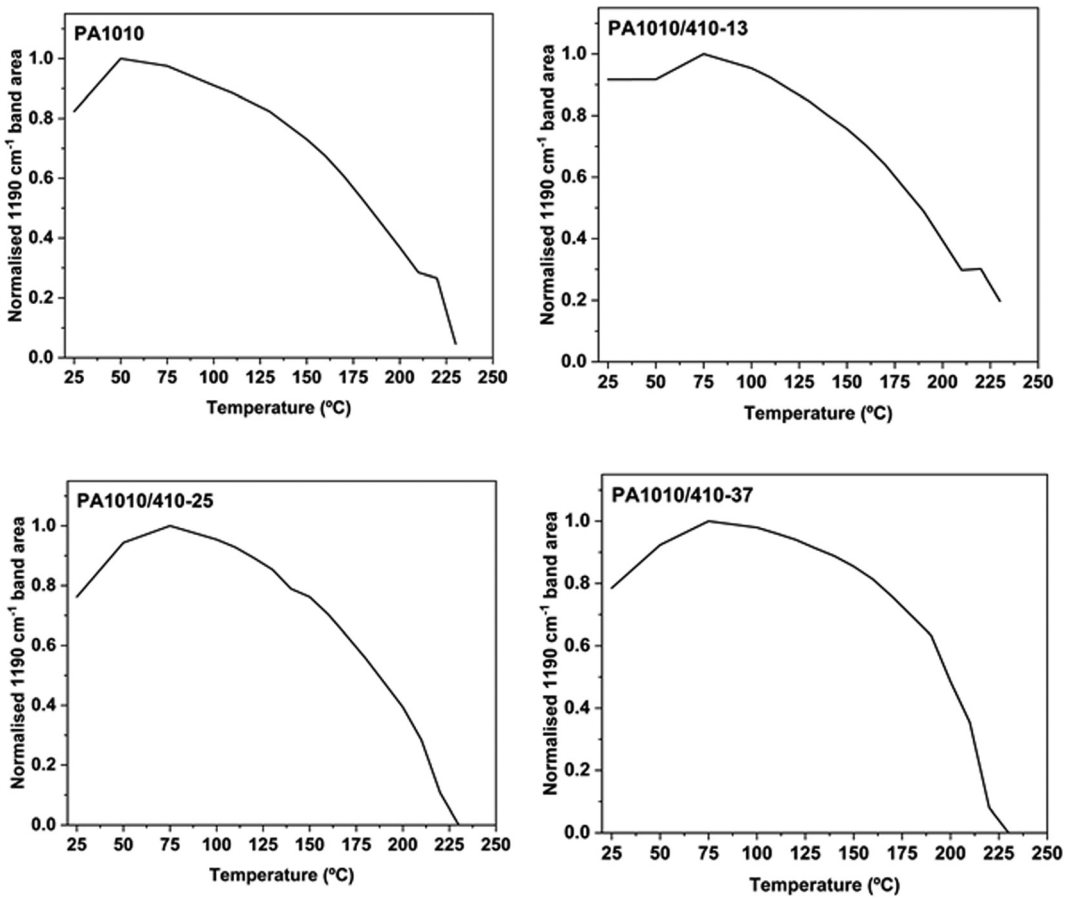

Fig. 10 Normalized area corresponding to 1190 cm^{-1} band of polyamide 1010 (PA1010) and copolyamides 410/1010: PA1010/410 with 12.5, 25 and 37.5 mol% nylon 410.

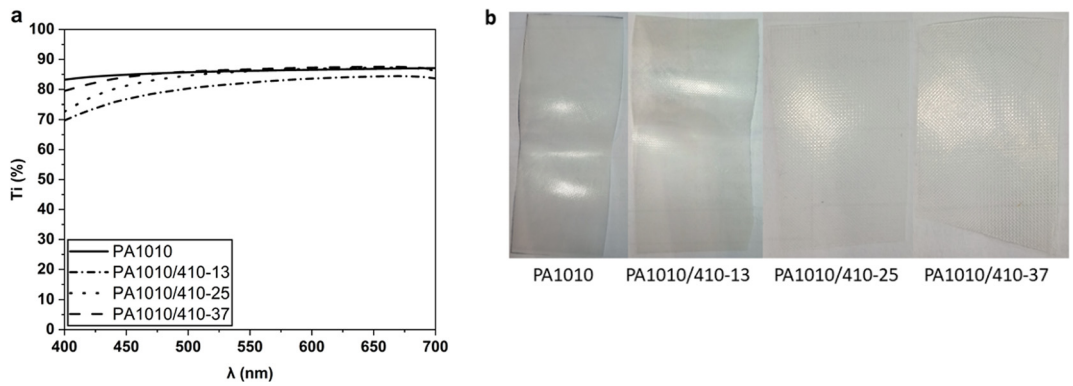

Fig. 11 (a) Spectral distribution curve of the percentage of internal transmittance (T_i) of polyamide 1010 (PA1010) and copolyamides 1010/410 (PA1010/410) films. (b) Images of the PA1010 and PA1010/410 films.

Table 3 Color parameters (L^*, a^*, b^*) hue angle (h^*_{ab}), color saturation or chroma (C^*_{ab}), and color difference (ΔE^*_{ab}) of polyamide 1010 (PA1010) and copolyamides 1010/410 (PA1010/410) films

Sample	L^*	a^*	b^*	C^*_{ab}	h^*_{ab}	ΔE^*_{ab}
PA 1010	87.5 ± 0.4^{a}	-1.2 ± 0.0^{a}	3.4 ± 0.1^{a}	3.6 ± 0.1^{a}	108.2 ± 0.7^{a}	—
PA1010/410-13	80.5 ± 1.5^{b}	-0.5 ± 1.1^{b}	16.7 ± 2.1^{b}	16.8 ± 2.0^{b}	92.2 ± 4.3^{b}	12.5 ± 0.5^{a}
PA1010/410-25	81.7 ± 1.7^{b}	-1.2 ± 1.2^{a}	22.0 ± 3.1^{c}	22.0 ± 3.0^{c}	92.5 ± 3.3^{b}	18.6 ± 0.7^{b}
PA1010/410-37	$84.6 \pm 0.3^{a,b}$	-2.7 ± 0.1^{c}	11.7 ± 0.5^{d}	11.4 ± 0.5^{d}	103.7 ± 0.3^{a}	9.2 ± 0.9^{c}

Different superscript letters ($^{a–d}$) indicate significant differences among formulations ($p < 0.05$).

 This journal is © The Royal Society of Chemistry 2025

Open Access Article. Published on 15 1447. Downloaded on 18/07/47 09:14:27 .
This article is licensed under a Creative Commons Attribution 3.0 Unported Licence.

color saturation or chroma (C^*_{ab}) of 11–22. The color variation results confirmed that the copolyamide films showed different colors than the homopolyamide film since, in all cases, $\Delta E^*_{ab} \geq 5$.

The mechanical properties of the PA1010/410 films were also evaluated to ascertain the effect of the putrescine content on their performance for food packaging applications. Results of the tensile tests are collated in Fig. 12. The tensile stress–strain curves of the PA1010 and PA1010/410 films taken at room temperature can be seen in Fig. 12a. One can observe that the progressive introduction of nylon 410-unit contents drastically changed the mechanical response of the bio-based polyamide films. Thus, whereas the mechanical properties of the PA1010 film correspond to a material with intermediate elasticity and high resistance but relatively low ductility, the PA1010/410 films presented lower mechanical strength but higher ductility. Fig. 12b–d respectively show the evolution of the tensile modulus (E), strength at yield (σ_y), and elongation at break (ε_b). In particular, the PA1010 films presented average values of E, σ_y, and ε_b of 1275 MPa, 53 MPa, and 18%, respectively. The introduction of low and medium contents of nylon 410, that is, 12.5 and 25 mol%, yielded to films with E, σ_y, and ε_b values in the 900–700 MPa, 45–40 MPa, and 40–20%, respectively. In any case, the most notably variation in the mechanical performance was seen PA1010/410 with 37.5 mol% nylon 410, which presented respective average values of E, σ_y, and ε_b values of 435 MPa, 31 MPa, and 135%. This result indicates that the latter copolyamide films is nearly 3 times less rigid and approximately 8 times more flexible that its homopolyamide film. In this regard, Lin *et al.*,[52] reported a significant enhancement in ductility for random copolyamide 56/66 (PA56/66) for 5N6C segments content of 30–70 mol%, which was ascribed to originate from the crystallinity decrease caused by the destruction of segment regularity by copolymerization. Similar results were attained by Ai *et al.*,[16] who observed that the toughness and flexibility of the bio-based copolyamides based on polyamide 10T and polyamide 56 significantly increased with the PA56 content. Thus, the variation of the mechanical performance as the 410-unit content increases, that is, reduction in strength but increase in flexibility, can be ascribed to the crystallinity reduction of the copolyamides. Therefore, the higher intermolecular chain mobility attained in the random PA1010/410 copolyamides confers sufficient freedom to better respond to externally applied strains.[53] Meanwhile, the chance of forming inter-chain entanglements between the crystalline and amorphous phases of copolyamides increases as the molecular chain mobility rises. These may act as stress transmitters during stretching to

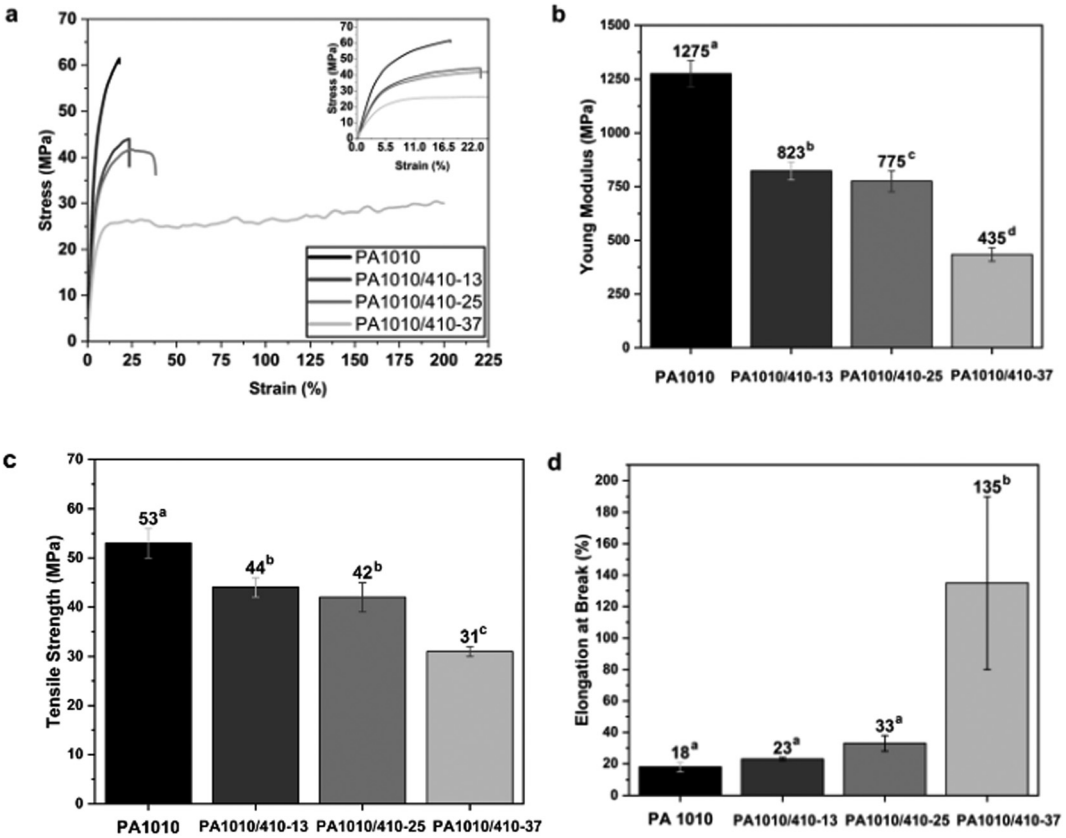

Fig. 12 (a) Typical tensile stress–strain curve of polyamide 1010 (PA1010) and copolyamides 1010/410 (PA1010/410) films. Evolution of the (b) tensile modulus (E), (c) tensile strength at yield (σ_y), and (d) elongation at break (ε_b). Different superscript letters ($^{a-d}$) indicate significant differences among formulations ($p < 0.05$).

Open Access Article. Published on 15 1447. Downloaded on 18/07/47 09:14:27 .
This article is licensed under a Creative Commons Attribution 3.0 Unported Licence.

enable the applied stress to be efficiently transferred within the sample, eliminating stress concentrations in weak regions within the copolyamides, such as spherulite boundaries and lamellae surfaces.[54,55] Therefore, the mechanical performance of these green nylon films varied according to their putrescine content, changing from highly resistant to significantly more ductile, which represents a competitive advantage to be applied in different food packaging systems, covering from rigid to flexible applications.

The barrier performance of the PA1010 and PA1010/410 films was also analyzed in terms of their permeability to water and limonene vapors and oxygen gas. Fig. 13 gathers the WVP, LP, and OP values of the bio-based polyamide films, all measured at 25 °C and 53% RH. One can observe that the WVP values increased progressively in the copolyamide films with increasing the putrescine content. This reduction in the water vapor barrier with the 410-unit content increase is related to both the decrease in crystallinity and in the CH_2/CONH ratio. The higher CONH densities per unit length of chain, resulting from the higher presence of the amide 410 segments, contributed to the development of a chemical structure that was more affected by water and, hence, by the moisture conditions. Thus, the WVP of PA1010 increased from 1.56 $\times 10^{-15}$ kg m m^{-2} Pa^{-1} s^{-1} up to 6.54 $\times 10^{-15}$ kg m m^{-2} Pa^{-1} s^{-1} for the PA1010/410 with 37.5 mol% of nylon 410. Similar values of permeability were observed by Nguyen *et al.*[56] These permeability values place the here-developed bio-based copolyamide films in between those of PA6 (2.06 $\times 10^{-14}$ kg m m^{-2} Pa^{-1} s^{-1} at 90% HR)[57] and PA12 (3.46 $\times 10^{-15}$ kg m m^{-2} Pa^{-1} s^{-1} at 85% HR)[58] and only one order of magnitude higher than high-water-vapor-barrier PP (7.26 $\times 10^{-16}$ kg m m^{-2} Pa^{-1} s^{-1} at 90% HR).[57] Therefore, these materials show great promise for applications in food environments where moderate or relatively high vapor-barrier performance is needed, such as meat packaging. One can further observe that the permeability to limonene, used habitually as standard to ascertain the barrier to aroma, was not significantly different ($p > 0.05$) among the bio-based polyamide film samples, with values in the 1.61–1.78 $\times 10^{-15}$ kg m m^{-2} Pa^{-1} s^{-1} range. These values are, for instance, notably lower than those observed for bio-based polyesters, such as PLA (3.3 $\times 10^{-15}$ kg m m^{-2} Pa^{-1} s^{-1}) or PHBV (1.0 $\times 10^{-14}$ kg m m^{-2} Pa^{-1} s^{-1}), all measured at 40% RH.[59] This further confirms the high potential of PA1010 and the PA1010/410 copolyamides, even as monolayer materials, with moisture and aroma resistance for sustainable food packaging applications.

In relation to oxygen, one can observe in Fig. 13c that the PA1010/410 films yielded values of OP in the 5.2–6.1 $\times 10^{-19}$

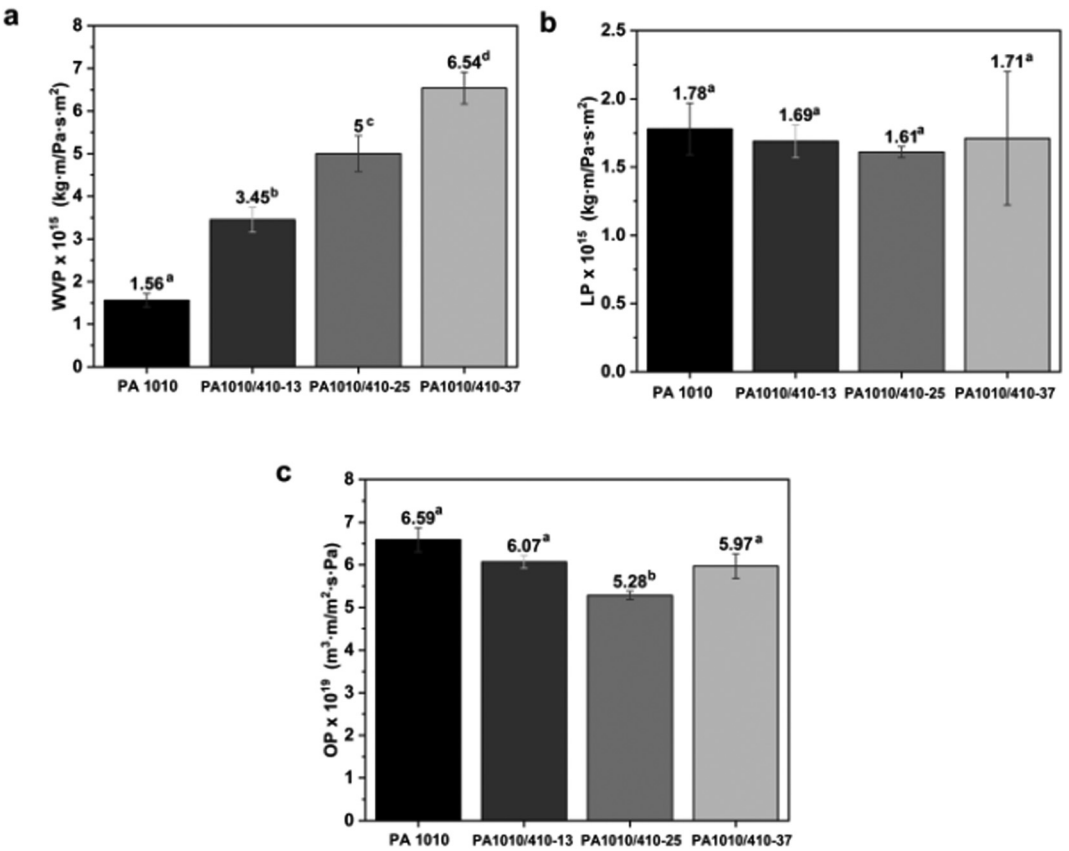

Fig. 13 (a) Water vapor permeability (WVP), (b) limonene permeability (LP), and (c) oxygen permeability (OP) of polyamide 1010 (PA1010) and copolyamides 1010/410 (PA1010/410) films measured at 25 °C and 53% relative humidity (RH). Different superscript letters ($^{a-d}$) indicate significant differences among formulations ($p < 0.05$).

 This journal is © The Royal Society of Chemistry 2025

Open Access Article. Published on 15 1447. Downloaded on 18/07/47 09:14:27 .
This article is licensed under a Creative Commons Attribution 3.0 Unported Licence.

m^3 m m^{-2} Pa^{-1} s^{-1} range at 53% RH. In all cases, these permeability values were lower than that of PA1010, which presented a value of 6.6×10^{-19} m^3 m m^{-2} Pa^{-1} s^{-1}. This permeability reduction, that is, oxygen barrier enhancement, was significantly attained ($p < 0.05$) in the case of PA1010/410-25, showing the lowest permeability with a value of 5.28×10^{-19} m^3 m m^{-2} Pa^{-1} s^{-1}. However, the film of copolyamide PA1010/410-37 presented a slightly but still significantly ($p < 0.05$) higher permeability value than the same copolyamide with 25 mol%. In this regard, the non-linear evolution of the oxygen barrier performance of the PA1010/410 copolyamides can be explained by the opposite effect induced by the introduction nylon 410-unit contents on the two distinct parameters affecting the permeability, that is, solubility, a thermodynamic parameter, and diffusivity, a kinetic one.[60] On the one hand, as opposite to WVP, the reduction in the CH_2/CONH ratio after the introduction of amide 4/10 segments yielded a progressive decrease in oxygen solubility in their glassy amorphous regions. On the other hand, the above-described reduction in the degree of crystallinity with the nylon 410-unit content increase impaired the permeability to oxygen of the copolyamides. In this regard, oxygen molecules with an effective radius of about 2 Å cannot diffuse through crystalline regions but can only permeate through amorphous regions with fractional free volumes larger than the molecules.[61] Thus, crystalline domains can both act as excluded volume for sorption of penetrant molecules decreasing solubility and form impermeable barriers for diffusion process increasing the average path length of these penetrant molecules. In any case, the oxygen barrier of PA1010/410 as well as PA1010 corresponds to an oxygen medium-barrier polymer, which is between the permeability of short-chain PA6, showing values in the 0.5–2.5 $\times 10^{-19}$ m^3 m m^{-2} Pa^{-1} s^{-1} range,[57] and long-chain PA12, in the 2.0–2.2 $\times 10^{-18}$ m^3 m m^{-2} Pa^{-1} s^{-1} range,[58] depending on the % RH.

3.4. Application for meat packaging purposes

Finally, the PA1010/410 film samples were used as lids on aluminum trays for packaging minced meat, which was stored for 11 days under refrigerated conditions, to determine their potential in food packaging. The food packaging performance of the bio-based copolyamide films were compared with petrochemical PP films. Table 4 shows the changes in pH, weight loss and color, according to the type of lid film and storage time. The pH value is an important indicator of meat quality, as it affects its color, water retention capacity, and flavor.[62] The minced meat showed an initial pH of 5.45 ± 0.05, in line with values previously reported for fresh minced meat samples.[63] Storage time and type of packaging both significantly affected the pH values of the samples ($p < 0.05$). The pH of minced meat packaged in PP samples increased from 5.45 to 7.14 on the eleventh day of storage. In general, the meat exhibited an increase in pH values indicating a degree of deterioration of the meat during protein breakdown giving rise to alkaline substances, such as amines.[64–66] The food samples packaged with PA1010/410 films had lower pH values than the ones with PP, showing no significant ($p > 0.05$) differences among the three PA1010/410-based samples on the last day of storage. Compared to the PP sample, the PA1010/410-based packaging was more effective in maintaining the pH of the meat samples. This result can be due to their enhanced oxygen and water vapor barrier properties, which affect oxidative and enzymatic reactions and microbial metabolism. Similar results were obtained in minced meat in gelatin–sodium alginate packaging film with date pits extract, showing pH values in the 6–7 range during the first 11 days.[63]

Weight loss is a very relevant factor for consumers and the meat industry as it is related to both meat quality and profitability.[67] The weight loss of the minced meat during storage is also reported in Table 4. Weight loss increased as a function of storage time in all meat samples. Thus, after six days of storage, the meat sample packaged in trays with the PP lid film presented the lowest weight loss (1.30%). This value was significantly lower ($p < 0.05$) than the values attained for the food

Table 4 Development of pH, weight loss and color parameters in terms of lightness (L^*), chroma (C^*_{ab}), hue (h^*_{ab}) and total color difference (ΔE^*_{ab}) of the cold-stored minced beef meat samples packaged in trays with the lid films of polypropylene (PP) and copolyamide 1010/410 (PA1010/410) with 12.5, 25, and 37.5 mol% nylon 410

	Storage time (days)		
Film	0	6	11
pH			
PP	$5.45 \pm 0.05^{a,1}$	$5.95 \pm 0.18^{a,2}$	$7.14 \pm 0.08^{a,3}$
PA1010/410-13	$5.45 \pm 0.05^{a,1}$	$5.78 \pm 0.11^{ab,2}$	$6.73 \pm 0.13^{b,3}$
PA1010/410-25	$5.45 \pm 0.05^{a,1}$	$5.65 \pm 0.06^{b,2}$	$6.62 \pm 0.09^{b,3}$
PA1010/410-37	$5.45 \pm 0.05^{a,1}$	$5.79 \pm 0.07^{a,2}$	$6.72 \pm 0.14^{b,3}$
Weight loss (%)			
PP	—	$1.30 \pm 0.009^{a,1}$	$1.47 \pm 0.002^{a,2}$
PA1010/410-13	—	$2.64 \pm 0.001^{b,1}$	$5.35 \pm 0.003^{b,2}$
PA1010/410-25	—	$2.81 \pm 0.010^{c,1}$	$5.75 \pm 0.002^{c,2}$
PA1010/410-37	—	$2.93 \pm 0.004^{d,1}$	$6.25 \pm 0.007^{d,2}$
L^*			
PP	$58.3 \pm 0.4^{a,1}$	$61.0 \pm 5.0^{ab,1}$	$54.6 \pm 0.3^{a,2}$
PA1010/410-13	$60.6 \pm 2.3^{a,1}$	$69.0 \pm 7.0^{ab,1,2}$	$64.2 \pm 0.04^{b,2}$
PA1010/410-25	$55.9 \pm 1.9^{b,1}$	$63.1 \pm 2.0^{b,2}$	$58.1 \pm 0.02^{c,3}$
PA1010/410-37	$56.9 \pm 2.8^{ab,1}$	$65.6 \pm 0.3^{a,2}$	$59.1 \pm 0.1^{d,1}$
C^*_{ab}			
PP	$7.0 \pm 0.3^{a,1}$	$7.7 \pm 0.9^{a,1}$	$9.8 \pm 0.3^{a,2}$
PA1010/410-13	$4.2 \pm 0.3^{b,1}$	$3.4 \pm 0.6^{b,1}$	$2.0 \pm 0.01^{b,2}$
PA1010/410-25	$5.9 \pm 1.7^{ab,1}$	$5.5 \pm 0.7^{c,1}$	$9.8 \pm 0.6^{a,2}$
PA1010/410-37	$6.6 \pm 0.1^{a,1}$	$5.3 \pm 0.2^{c,2}$	$7.5 \pm 0.2^{c,3}$
h^*_{ab}			
PP	$24 \pm 0.09^{a,1}$	$78 \pm 0.8^{a,2}$	$78 \pm 1.5^{a,2}$
PA1010/410-13	$34 \pm 0.7^{b,1}$	$76 \pm 1.8^{a,2}$	$69 \pm 0.05^{b,3}$
PA1010/410-25	$22 \pm 1.7^{c,1}$	$70 \pm 2.3^{b,2}$	$72 \pm 1.1^{c,2}$
PA1010/410-37	$23 \pm 0.1^{c,1}$	$61 \pm 0.3^{c,2}$	$72 \pm 0.4^{c,3}$
ΔE^*_{ab}			
PP	—	$3.6 \pm 0.7^{a,1}$	$5.3 \pm 0.3^{a,2}$
PA1010/410-13	—	$1.2 \pm 0.1^{b,1}$	$4.6 \pm 0.2^{b,2}$
PA1010/410-25	—	$1.7 \pm 0.2^{c,1}$	$3.1 \pm 0.3^{c,2}$
PA1010/410-37	—	$2.3 \pm 0.2^{d,1}$	$4.7 \pm 0.5^{b,2}$

Different superscript letters ($^{a–d}$) within the same column indicate significant differences among formulations ($p < 0.05$). Different superscript numbers ($^{1–3}$) within the same row for each parameter and sample indicate significant differences between the three storage times ($p < 0.05$).

Open Access Article. Published on 15 1447. Downloaded on 18/07/47 09:14:27 .
This article is licensed under a Creative Commons Attribution 3.0 Unported Licence.

samples packaged with the PA1010/410 films, which were 2.64%, 2.81%, and 2.93% for PA1010/410 with 12.5, 25, and 37.5 mol% nylon 410, respectively. At the end of storage (day 11), the weight loss values were 1.47%, 5.35%, 5.75%, and 6.25% for the meat samples packaged in trays with lid films of PP, PA1010/410-13, PA1010/410-25, and PA1010/410-37, respectively. Therefore, the PP-based film packaging provided a significantly ($p < 0.05$) lower weight loss during storage of the minced meat samples, below 2%. This weight variation among the packaged samples is consistent with the water vapor barrier of the PP film and the different PA1010/410 films. In this regard, one should consider that, during storage, a natural phenomenon of water loss occurs from the intramuscular fluid leakage from the cut surface of minced beef meat.[68] Therefore, water of this exudate permeated at different levels, directly correlating with the observed weight loss values. Furthermore, according to Huff-Lonergan *et al.*,[69] the water holding capacity of meat reaches its minimum value when muscle pH value is approximately 5.3, near the isoelectric point of meat proteins. As stated before, this pH value was closer to ones reached in the meat packaged with the PA1010/410 films. Similar results were reported by Nur Hanani *et al.*,[70] who developed gelatin-based active packaging films with silver–kaolinite and studied the weight loss of beef packaged in different systems reaching values of 2–3% at 6 days of storage in active cling films. Hernández-García *et al.*,[27] also reported results of weight loss in minced pork meat packaged in trays with lid films of PHBV reinforced with micro-fibrillated cellulose, reaching values of 1.5–2% after seven days of storage in cold storage conditions at 5 °C.

Meat surface color is an important visual indicator of meat quality that directly influences consumer acceptability.[71] Thus, the evolution of chromatic parameters (L^*, C^*_{ab}, h^*_{ab}) and total color difference (ΔE^*_{ab}) of minced meat with respect to the initial values ($t = 0$) was analyzed. During storage, the meat samples showed significant differences ($p < 0.05$) in lightness, chroma, and hue as a function of the type of lid film used for the food tray. One can observe that the meat samples packaged with the PA1010/410 films showed lower total color difference, expressed as ΔE, than the food sample packaged using the PP film. As similar to weight loss, color variation of the meat samples was also directly related to barrier properties of the films. In particular, the fully bio-based copolyamides were able to provide lower color differences due to their lower oxygen-barrier capacity than PP. In this regard, increases in lightness, chroma, and hue values result from myoglobin and lipid oxidation, which are known to lead meat discoloration or yellowing due to increased oxymyoglobin and metamyoglobin.[72] It is also worth noting that, after 11 days of storage, the total color differences of the meat samples packaged in all the PA1010/410-based trays did not positively exceed the usual tolerance limit for food products, whereas the meat samples packaged using PP was over the 5-unit level ($\Delta E < 5$).[73] Therefore, an improved color preservation was successfully attained in the samples packaged in PA1010/410 films, increasing for the samples with the lowest OTR values. In particular, the meat packaged with the PA1010/410-25 film was the sample that best preserved the color, attributed to the fact that it was the sample with the highest oxygen barrier and reduced oxidative processes.

Fig. 14 shows the microbial counts for TCC, LAB, and TVC of minced meat packaged in the food trays prepared with lid films of PA1010/410 and PP films. As recently reported,[25,74] the meat samples showed continuous microbial growth during storage, independent of the packaging type. Coliform bacteria are meat quality indicator microorganisms.[75] As shown in Fig. 14a, the evolution of TCC was significantly affected ($p < 0.05$) by film type and storage time. Then, microbial counts of the meat samples packaged with the PP film increased from 1.94 to 5.31 log CFU per g, during the first six days, and to 6.91 log CFU per g at the end of storage (11 days). Similarly, counts increased in the meat samples packaged with the PA1010/410 films to 4.68, 4.13, and 4.42 log CFU per g, during the first week of storage, and to 5.99, 5.43, and 5.70 log CFU per g at the end of storage, for PA1010/410-13, PA1010/410-25, and PA1010/410-37, respectively, showing significant differences among the samples ($p < 0.05$). These results successfully correlated with the pH trend reported in Table 4. Moreover, the resulting profile of bacterial growth achieved in this packaged meat was in the range of those reported for PA1010 films that preserved pork fillet samples for one week under refrigeration conditions.[47]

Furthermore, LAB are predominant in vacuum-packed meat and meat products and pose a threat to the integrity of the food product during storage time due to their fermentation.[76] Fig. 14b shows that the initial bacteria count in the minced meat samples was 2.0 log CFU per g, in the range reported in other studies.[77] Thus, LAB counts were also significantly affected by packaging type and storage. At the end of storage, food samples packaged using PP showed the highest microbial growth, 6.33 log CFU per g. In contrast, the meat samples packaged with the PA1010/410 lid films showed lower microbial growth. In particular, counts of 5.62, 4.25 and 5.10 log CFU per g were respectively attained for PA1010/410-13, PA1010/410-25, and PA1010/410-37 with significant differences among the samples ($p < 0.05$). Therefore, the lowest bacterial growth was achieved for the food packaging based on PA1010/410-25, showing a 2.08-log reduction at the end of storage with respect to the meat packaged with PP film. These results were also consistent with the pH data obtained in Table 4 as well as with the lowest oxygen permeability of the PA1010/410 films, successfully yielding the least microbial growth. In this regard, Hernández-García *et al.*,[26] obtained similar results for the packaging of pork fillets with starch-polyester bilayer films with different phenolic acids.

The growth of TVC was also finally determined to evaluate the quality and safety of meat, which is a standard to identify the degree of contamination and processing conditions of meat.[78] In all samples, as seen in Fig. 14c, TVC increased both at 6 days and at the end of storage (11 days), which is mainly related to the proliferation of psychrotrophic bacteria.[79] One can observe that counts increased from approximately 1.69 log CFU per g to 5.95 log CFU per g in the minced meat packaged

 This journal is © The Royal Society of Chemistry 2025

Open Access Article. Published on 15 1447. Downloaded on 18/07/47 09:14:27 .
This article is licensed under a Creative Commons Attribution 3.0 Unported Licence.

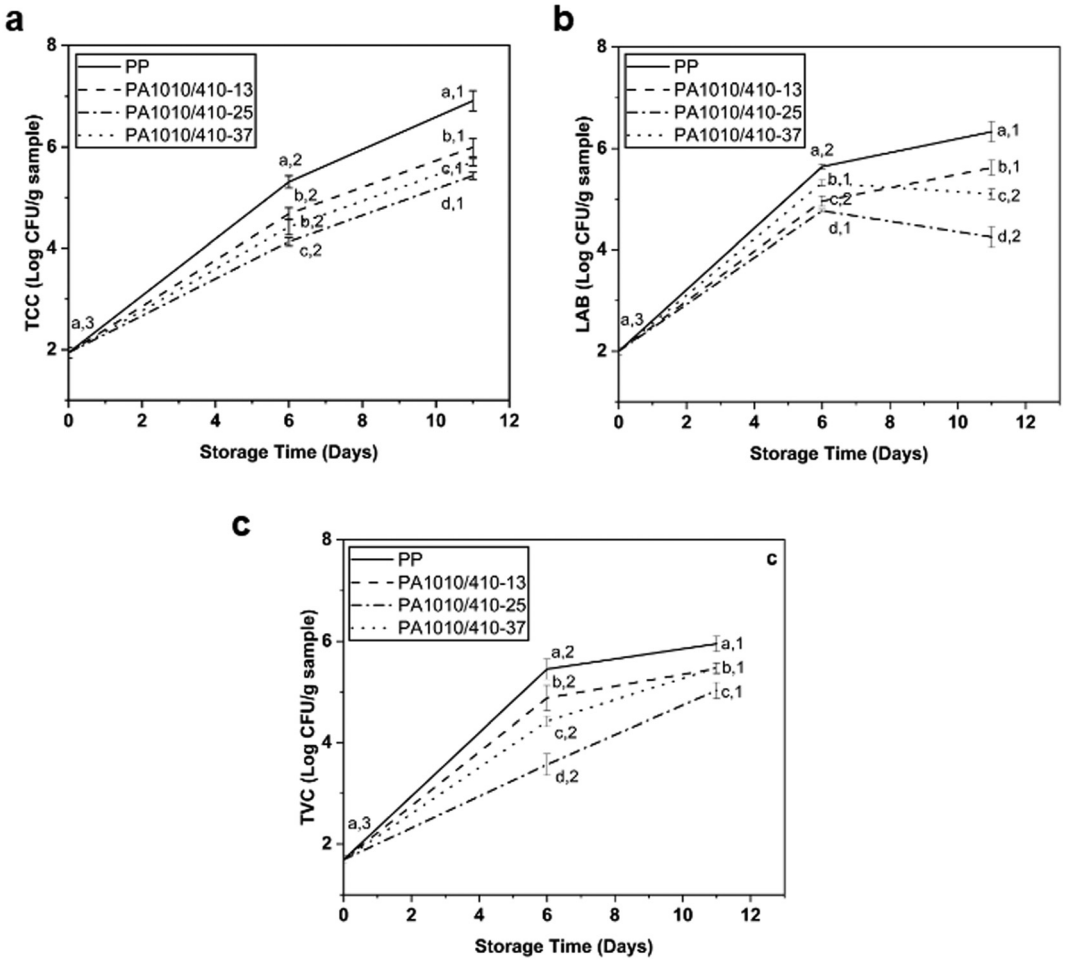

Fig. 14 Changes in microbial counts: (a) total coliform counts (TCC), (b) lactic acid bacteria (LAB) and (c) total viable counts (TVC) in minced beef meat samples packaged in trays with the lid films of polypropylene (PP) and PA1010/410 with 12.5, 25 and 37.5 mol% nylon 410 during storage. Different superscript letters ($^{a-d}$) within the same storage time indicate significant differences among formulations ($p < 0.05$). Different superscript numbers ($^{1-3}$) within the same parameter and sample indicate significant differences between the three storage times ($p < 0.05$).

in trays with the PP film used as lids. As for the other bacteria counts, significant differences ($p < 0.05$) were observed in the different samples and during storage. The growth in the meat packaged in the PA1010/410-based trays was lower than that observed in the food packaging with PP, being the PA1010/410-25 film sample the one providing the lowest growth with a value of 5.03 log CFU per g at the end of storage. In this regard, the European Commission Regulation on microbiological criteria for mechanically separated fresh pork meat states that the maximum acceptable level of total viable bacteria is 5 log CFU per g.[78] According to the bacteria counts obtained in this study, minced meat can be safely stored under refrigerated conditions at 5 °C in the trays using PP lid films for only up to 5 days, while meat samples packaged using PA1010/410 lid films should not exceed 9 days under refrigerated conditions (5 °C). Thus, the use of these green nylons in meat packaging can represent a shelf-life extension of up to 4 days in comparison of monolayer films based on petrochemical polyolefins, therby contributing to a reduction in food waste.

4. Conclusions

The present study reports on the synthesis, characterization, and food packaging application of fully bio-based PA1010/410 obtained by polycondensation reaction from different molar contents of "nylon salts" derived from renewable putrescine, decamethylenediamine, and sebacic acid monomers. The partial substitution of decamethylenediamine by putrescine turned the previously developed homopolyamide PA1010 into random copolyamides with moderate M_W that are mechanically more flexible, melt and hence can seal at lower temperatures, and also present medium-to-high oxygen barrier. The physical properties of the newly developed bio-based copolyamides were related to their chemical structure and crystalline characteristics. Within the range of molar compositions studied, it was observed that these copolyamides present lower crystallinity and an isodimorphic behavior with partial comonomer inclusion, displaying a "pseudo-eutectic" region for intermediate putrescine compositions. Furthermore, when

Open Access Article. Published on 15 1447. Downloaded on 18/07/47 09:14:27 .
This article is licensed under a Creative Commons Attribution 3.0 Unported Licence.

applied in the form of lid films, these novel green nylons demonstrated to be effective in preserving the physicochemical and microbiological quality of meat, outperforming the PP polyolefin at the refrigerated storage conditions of 5 °C. Therefore, by means of copolymerization using different putrescine contents, the properties of these green nylon can be adapted for the targeted food packaging application. Whereas the homopolyamide is of most interest for rigid food packaging where higher thermal resistance and water barrier are needed, the copolyamides are advantageous for food packaging applications that require better processability, lower SIT, and higher flexibility. For instance, the here-developed copolyamides can be regarded as great candidates for use in paper-based multilayer structures that can be easily sealed as external layers to provide water resistance and aroma and oxygen barrier. Future studies will be focused on analyzing other molar ratio ranges to determine the exact composition of the pseudo-eutectic point and the level of comonomer inclusion. Moreover, other works will deal with their application in food packaging multilayers as well as methodologies to recycle them within current Circular Economy scenarios.

Author contributions

M. Pacheco-Romeralo: conceptualization, methodology, validation, formal analysis, writing – original draft. E. Hernández-García: methodology, validation, formal analysis. A. Martínez de Ilarduya: methodology, validation, formal analysis, writing – review & editing. R. Janani: methodology, validation, formal analysis. C. Sammon: methodology, validation, formal analysis. S. Torres-Giner: conceptualization, methodology, validation, formal analysis, writing – review & editing, supervision, project administration, funding acquisition. All authors have read and agreed to the published version of the manuscript.

Conflicts of interest

There are no conflicts to declare.

Data availability

Research data will be available in our Institutional Repository RiuNet: https://riunet.upv.es/home.

Acknowledgements

This research was supported by PID2021-128749OB-C33 from the Spanish Ministry of Science and Innovation (MICI) and INNVA1/2024/106 and EDGJID/2021/290 both from the Generalitat Valenciana (GVA). Sergio Torres-Giner acknowledges MICI for his "Ramón y Cajal" contract (RYC2019-027784-I) for funding and financial support during the research stay at Sheffield Hallam University. Eva Hernández-García thanks the support of her "Margarita Salas" Postdoctoral Fellowship funded by the European Union-Next Generation EU program.

References

1 S. Torres-Giner, K. J. Figueroa-Lopez, B. Melendez-Rodriguez, C. Prieto, M. Pardo-Figuerez and J. M. Lagaron, Emerging Trends in Biopolymers for Food Packaging, in *Sustainable Food Packaging Technology*, Wiley, 2021, pp. 1–33. DOI: 10.1002/9783527820078.ch1.

2 K. Y. Perera, A. K. Jaiswal and S. Jaiswal, Biopolymer-Based Sustainable Food Packaging Materials: Challenges, Solutions, and Applications, *Foods*, 2023, **12**(12), 2422, DOI: 10.3390/foods12122422.

3 S. P. Bangar, W. S. Whiteside, A. O. Ashogbon and M. Kumar, Recent advances in thermoplastic starches for food packaging: A review, *Food Packag. Shelf Life*, 2021, **30**, 100743, DOI: 10.1016/j.fpsl.2021.100743.

4 S. Paudel, S. Regmi and S. Janaswamy, Effect of glycerol and sorbitol on cellulose-based biodegradable films, *Food Packag. Shelf Life*, 2023, **37**, 101090, DOI: 10.1016/j.fpsl.2023.101090.

5 S. Torres-Giner, L. Gil, L. Pascual-Ramírez and J. Garde-Belza, *Packaging: Food Waste Reduction*, 2018, pp. 1990–2009. DOI: 10.4324/9781351019422-120054093.

6 W. Grzebieniarz, D. Biswas, S. Roy and E. Jamróz, Advances in biopolymer-based multi-layer film preparations and food packaging applications, *Food Packag. Shelf Life*, 2023, **35**, 101033, DOI: 10.1016/j.fpsl.2023.101033.

7 M. Pervaiz, M. Faruq, M. Jawaid and M. Sain, Polyamides: Developments and Applications Towards Next-Generation Engineered Plastics, *Curr. Org. Synth.*, 2017, **14**(2), 146–155, DOI: 10.2174/1570179413666160831112159.

8 M. A. Del Nobile, G. G. Buonocore, L. Palmieri, A. Aldi and D. Acierno, Moisture transport properties of polyamides copolymers intended for food packaging applications, *J. Food Eng.*, 2002, **53**(3), 287–293, DOI: 10.1016/S0260-8774(01)00167-4.

9 S. Kind, S. Neubauer, J. Becker, *et al.*, From zero to hero – Production of bio-based nylon from renewable resources using engineered Corynebacterium glutamicum, *Metab. Eng.*, 2014, **25**, 113–123, DOI: 10.1016/j.ymben.2014.05.007.

10 R. J. H. Navasingh, M. K. Gurunathan, M. P. Nikolova and J. B. Królczyk, Sustainable Bioplastics for Food Packaging Produced from Renewable Natural Sources, *Polymers*, 2023, **15**(18), 3760, DOI: 10.3390/polym15183760.

11 D. Ogunniyi, Castor oil: A vital industrial raw material, *Bioresour. Technol.*, 2006, **97**(9), 1086–1091, DOI: 10.1016/j.biortech.2005.03.028.

12 E. Hernández-García, M. Pacheco-Romeralo, L. Pascual-Ramírez, M. Vargas and S. Torres-Giner, Synthesis and characterization of polyamide 1010 and evaluation of its cast-extruded films for meat preservation, *Food Packag.*

 This journal is © The Royal Society of Chemistry 2025

Open Access Article. Published on 15 1447. Downloaded on 18/07/47 09:14:27 .
This article is licensed under a Creative Commons Attribution 3.0 Unported Licence.

Shelf Life, 2023, **36**, 101058, DOI: 10.1016/j.fpsl.2023.101058.

13 N. A. Jones, E. D. T. Atkins, M. J. Hill, S. J. Cooper and L. Franco, Chain-folded lamellar crystals of aliphatic polyamides. Investigation of nylons 4 8, 4 10, 4 12, 6 10, 6 12, 6 18 and 8 12, *Polymer*, 1997, **38**(11), 2689–2699, DOI: 10.1016/S0032-3861(97)85603-0.

14 B. Bamps, M. Buntinx and R. Peeters, Seal materials in flexible plastic food packaging: A review, *Packag. Technol. Sci.*, 2023, **36**(7), 507–532, DOI: 10.1002/pts.2732.

15 L. Quiles-Carrillo, N. Montanes, T. Boronat, R. Balart and S. Torres-Giner, Evaluation of the engineering performance of different bio-based aliphatic homopolyamide tubes prepared by profile extrusion, *Polym. Test.*, 2017, **61**, 421–429, DOI: 10.1016/j.polymertesting.2017.06.004.

16 T. Ai, G. Zou, W. Feng, *et al.*, Synthesis and properties of biobased copolyamides based on polyamide 10T and polyamide 56 through one-pot polymerization, *New J. Chem.*, 2021, **45**(32), 14677–14686, DOI: 10.1039/D1NJ02330F.

17 S. Kind and C. Wittmann, Bio-based production of the platform chemical 1, 5-diaminopentane, *Appl. Microbiol. Biotechnol.*, 2011, **91**(5), 1287–1296, DOI: 10.1007/s00253-011-3457-2.

18 Z. Qian, X. Xia and S. Y. Lee, Metabolic engineering of *Escherichia coli* for the production of putrescine: A four carbon diamine, *Biotechnol. Bioeng.*, 2009, **104**(4), 651–662, DOI: 10.1002/bit.22502.

19 L. Jasinska, M. Villani, J. Wu, *et al.*, Novel, Fully Biobased Semicrystalline Polyamides, *Macromolecules*, 2011, **44**(9), 3458–3466, DOI: 10.1021/ma200256v.

20 S.-P. Rwei, P. Ranganathan, W.-Y. Chiang and Y.-H. Lee, Synthesis and characterization of copolyamides derived from novel aliphatic bio–based diamine, *J. Appl. Polym. Sci.*, 2018, **135**(48), 46878, DOI: 10.1002/app.46878.

21 S. M. Aharoni, F. G. Cilurso and J. M. Hanrahan, Trifluoroethanol/chloroalkane mixtures: Excellent novel solvents for aliphatic polyamides, *J. Appl. Polym. Sci.*, 1985, **30**(6), 2505–2525, DOI: 10.1002/app.1985.070300618.

22 K. Wudy and D. Drummer, Aging effects of polyamide 12 in selective laser sintering: Molecular weight distribution and thermal properties, *Addit. Manuf.*, 2019, **25**, 1–9, DOI: 10.1016/j.addma.2018.11.007.

23 M. Wojdyr, Fityk: a general-purpose peak fitting program, *J. Appl. Crystallogr.*, 2010, **43**(5), 1126–1128, DOI: 10.1107/S0021889810030499.

24 A. Agüero, M. d. C. Morcillo, L. Quiles-Carrillo, *et al.*, Study of the Influence of the Reprocessing Cycles on the Final Properties of Polylactide Pieces Obtained by Injection Molding, *Polymers*, 2019, **11**(12), 1908, DOI: 10.3390/polym11121908.

25 J. Andrade, C. González-Martínez and A. Chiralt, Antimicrobial PLA-PVA multilayer films containing phenolic compounds, *Food Chem.*, 2022, **375**, 131861, DOI: 10.1016/j.foodchem.2021.131861.

26 E. Hernández-García, M. Vargas and S. Torres-Giner, Quality and Shelf-Life Stability of Pork Meat Fillets Packaged in Multilayer Polylactide Films, *Foods*, 2022, **11**(3), 426, DOI: 10.3390/foods11030426.

27 E. Hernández-García, A. Chiralt, M. Vargas and S. Torres-Giner, Lid Films of Poly(3-hydroxybutyrate-*co*-3-hydroxyvalerate)/Microfibrillated Cellulose Composites for Fatty Food Preservation, *Foods*, 2023, **12**(2), 375, DOI: 10.3390/foods12020375.

28 X. Cui, Z. Liu and D. Yan, Synthesis and characterization of novel even–odd nylons based on undecanedioic acid, *Eur. Polym. J.*, 2004, **40**(6), 1111–1118, DOI: 10.1016/j.eurpolymj.2003.12.021.

29 Y. Li, G. Zhang and D. Yan, Synthesis and crystallization behavior of nylon 12,14. I, Preparation and melting behavior, *J. Appl. Polym. Sci.*, 2003, **88**(6), 1581–1589, DOI: 10.1002/app.11826.

30 C. Koning, L. Teuwen, R. de Jong, G. Janssen and B. Coussens, Polyamides 4.10 and 4.12 and their Isomers, *High Perform. Polym.*, 1999, **11**(4), 387–394, DOI: 10.1088/0954-0083/11/4/304.

31 C. Marcoaldi, M. Pardo-Figuerez, C. Prieto, *et al.*, Electrospun Multilayered Films Based on Poly(3-hydroxybutyrate-*co*-3-hydroxyvalerate), Copolyamide 1010/1014, and Electrosprayed Nanostructured Silica, *Nanomaterials*, 2023, **13**(6), 972, DOI: 10.3390/nano13060972.

32 L. Quiles-Carrillo, N. Montanes, V. Fombuena, R. Balart and S. Torres-Giner, Enhancement of the processing window and performance of polyamide 1010/bio–based high–density polyethylene blends by melt mixing with natural additives, *Polym. Int.*, 2020, **69**(1), 61–71, DOI: 10.1002/pi.5919.

33 M. Winnacker and B. Rieger, Biobased Polyamides: Recent Advances in Basic and Applied Research, *Macromol. Rapid Commun.*, 2016, **37**(17), 1391–1413, DOI: 10.1002/marc.201600181.

34 Z. Zhang, W. Liu, H. Liu, *et al.*, Temperature and deformation dependence of structural evolution in polyamide 1010, *J. Polym. Res.*, 2019, **26**(12), 284, DOI: 10.1007/s10965-019-1955-6.

35 J. Wang, G. Zhao and Y. Zhou, Stretching crystallization behavior and brill transition of nylon 1010, *Chem. Res. Chin. Univ.*, 2011, **32**, 1225–1230.

36 J. L. J. van Velthoven, L. Gootjes, B. A. J. Noordover and J. Meuldijk, Bio-based, amorphous polyamides with tunable thermal properties, *Eur. Polym. J.*, 2015, **66**, 57–66, DOI: 10.1016/j.eurpolymj.2015.01.040.

37 M. Firdaus and M. A. R. Meier, Renewable polyamides and polyurethanes derived from limonene, *Green Chem.*, 2013, **15**(2), 370–380, DOI: 10.1039/C2GC36557J.

38 Z. Wang, G. Hu, J. Zhang, J. Xu and W. Shi, Isothermal Crystallization Kinetics of Nylon 10T and Nylon 10T/1010 Copolymers: Effect of Sebacic Acid as a Third Comonomer, *J. Wuhan Univ. Technol., Mater. Sci. Ed.*, 2018, **33**(5), 1247–1255, DOI: 10.1007/s11595-018-1959-9.

39 S. P. Rwei, P. Ranganathan and Y. H. Lee, Isothermal Crystallization Kinetics Study of Fully Aliphatic PA6 Copolyamides: Effect of Novel Long-Chain Polyamide Salt

Open Access Article. Published on 15 1447. Downloaded on 18/07/47 09:14:27 .
This article is licensed under a Creative Commons Attribution 3.0 Unported Licence.

as a Comonomer, *Polymers*, 2019, **11**(3), 472, DOI: 10.3390/polym11030472.

40 *Vibrational Spectra and Structure*, ed. J. R. Durig, Marcel Dekker, New York, 1972–2000, vol. 24.

41 Y. Yoshioka, K. Tashiro and C. Ramesh, Structural change in the Brill transition of Nylon m/n (2) conformational disordering as viewed from the temperature-dependent infrared spectral measurements, *Polymer*, 2003, **44**(20), 6407–6417, DOI: 10.1016/S0032-3861(03)00593-7.

42 C. Yan, L. Hao, L. Xu and Y. Shi, Preparation, characterisation and processing of carbon fibre/polyamide-12 composites for selective laser sintering, *Compos. Sci. Technol.*, 2011, **71**(16), 1834–1841, DOI: 10.1016/j.compscitech.2011.08.013.

43 A. L. Margolin, N. V. Vorontsov, T. V. Monakhova and A. A. Popov, Thermal oxidation of blends of polypropylene and polyamide 6/66. Effect of inhibition, *Polym. Degrad. Stab.*, 2024, **220**, 110627, DOI: 10.1016/j.polymdegradstab.2023.110627.

44 R. A. Pérez-Camargo, I. Arandia, M. Safari, *et al.*, Crystallization of isodimorphic aliphatic random copolyesters: Pseudo-eutectic behavior and double-crystalline materials, *Eur. Polym. J.*, 2018, **101**, 233–247, DOI: 10.1016/j.eurpolymj.2018.02.037.

45 C. S. Moran, A. Barthelon, A. Pearsall, V. Mittal and J. R. Dorgan, Biorenewable blends of polyamide–4,10 and polyamide–6,10, *J. Appl. Polym. Sci.*, 2016, **133**(45), 43626, DOI: 10.1002/app.43626.

46 P. Wu, *Two-dimensional correlation analysis of variable-temperature Fourier-transform near-infrared spectra of an amorphous polyamide*, 2003. DOI: 10.1063/1.1302844.

47 E. Hernández-García, P. A. V. Freitas, P. Zomeño, C. González-Martínez and S. Torres-Giner, Multilayer Sheets Based on Double Coatings of Poly(3-hydroxybutyrate-*co*-3-hydroxyvalerate) on Paper Substrate for Sustainable Food Packaging Applications, *Appl. Sci.*, 2022, **13**(1), 179, DOI: 10.3390/app13010179.

48 L. Sun, R. Zhu, H. Hu, *et al.*, Study on yellowing mechanism and inhibiting technology based on amide salts modified polyester, *Text. Res. J.*, 2023, **93**(7–8), 1824–1839, DOI: 10.1177/00405175221137351.

49 D. Fromageot, A. Roger and J. Lemaire, Thermooxidation yellowing of aliphatic polyamides, *Angew. Makromol. Chem*, 1989, **170**(1), 71–85, DOI: 10.1002/apmc.1989.051700105.

50 S. Zhang and J. Ma, Improvement of color value of bio-based polyamide 56 fibers, *e-Polymers*, 2018, **18**(1), 91–95, DOI: 10.1515/epoly-2017-0079.

51 P. V. Nethra, K. V. Sunooj, B. Aaliya, *et al.*, Critical factors affecting the shelf life of packaged fresh red meat – A review, *Meas.: Food*, 2023, **10**, 100086, DOI: 10.1016/j.meafoo.2023.100086.

52 N. Lin, Z. Wang, H. Kang, X. Hao and R. Liu, Synthesis and characterizations of random copolyamide PA(56-co-66): Excellent toughness and transparency, *Polymer*, 2024, **307**, 127271, DOI: 10.1016/j.polymer.2024.127271.

53 R. Zhu, L. Sun, H. Hu, *et al.*, Effect of comonomer loading on the thermal and mechanical properties of biobased copolyamides PA6/PA56, *Polymer*, 2024, **302**, 127078, DOI: 10.1016/j.polymer.2024.127078.

54 A. G. McDermott, P. J. DesLauriers, J. S. Fodor, R. L. Jones and C. R. Snyder, Measuring Tie Chains and Trapped Entanglements in Semicrystalline Polymers, *Macromolecules*, 2020, **53**(13), 5614–5626, DOI: 10.1021/acs.macromol.0c00132.

55 M. Polińska, A. Rozanski, A. Galeski and J. Bojda, The Modulus of the Amorphous Phase of Semicrystalline Polymers, *Macromolecules*, 2021, **54**(19), 9113–9123, DOI: 10.1021/acs.macromol.1c01576.

56 P. H. Nguyen, S. Spoljaric and J. Seppälä, Redefining polyamide property profiles via renewable long-chain aliphatic segments: Towards impact resistance and low water absorption, *Eur. Polym. J.*, 2018, **109**, 16–25, DOI: 10.1016/j.eurpolymj.2018.08.057.

57 J. M. Lagarón, Multifunctional and nanoreinforced polymers for food packaging, in *Multifunctional and Nanoreinforced Polymers for Food Packaging*, Elsevier, 2011, pp. 1–28. DOI: 10.1533/9780857092786.1.

58 L. W. McKeen, Polyamides (Nylons), in *Film Properties of Plastics and Elastomers*, Elsevier, 2017, pp. 187–227. DOI: 10.1016/B978-0-12-813292-0.00008-3.

59 L. Quiles-Carrillo, N. Montanes, J. M. Lagaron, R. Balart and S. Torres-Giner, In Situ Compatibilization of Biopolymer Ternary Blends by Reactive Extrusion with Low-Functionality Epoxy-Based Styrene–Acrylic Oligomer, *J. Polym. Environ.*, 2019, **27**(1), 84–96, DOI: 10.1007/s10924-018-1324-2.

60 V. M. Litvinov, O. Persyn, V. Miri and J. M. Lefebvre, Morphology, Phase Composition, and Molecular Mobility in Polyamide Films in Relation to Oxygen Permeability, *Macromolecules*, 2010, **43**(18), 7668–7679, DOI: 10.1021/ma1014403.

61 J. Wu, Y. Huang, H. Li, J. Runt and J. Yeh, Properties of polyamide 6,10/poly(vinyl alcohol) blends and impact on oxygen barrier performance, *Polym. Int.*, 2018, **67**(4), 453–462, DOI: 10.1002/pi.5528.

62 U. S. Geletu, M. A. Usmael, Y. Y. Mummed and A. M. Ibrahim, Quality of Cattle Meat and Its Compositional Constituents, *Vet. Med. Int.*, 2021, **2021**, 1–9, DOI: 10.1155/2021/7340495.

63 K. Elhadef, M. Chaari, S. Akermi, *et al.*, Gelatin-sodium alginate packaging film with date pits extract: An eco-friendly packaging for extending raw minced beef shelf life, *Meat Sci.*, 2024, **207**, 109371, DOI: 10.1016/j.meatsci.2023.109371.

64 A. Pacquit, K. Lau, H. Mclaughlin, J. Frisby, B. Quilty and D. Diamond, Development of a volatile amine sensor for the monitoring of fish spoilage, *Talanta*, 2006, **69**(2), 515–520, DOI: 10.1016/j.talanta.2005.10.046.

65 S. Smaoui, A. B. Hsouna, A. Lahmar, *et al.*, Bio-preservative effect of the essential oil of the endemic Mentha piperita used alone and in combination with BacTN635 in stored

 This journal is © The Royal Society of Chemistry 2025

Open Access Article. Published on 15 1447. Downloaded on 18/07/47 09:14:27 .
This article is licensed under a Creative Commons Attribution 3.0 Unported Licence.

minced beef meat, *Meat Sci.*, 2016, **117**, 196–204, DOI: 10.1016/j.meatsci.2016.03.006.

66 D. Daniloski, A. T. Petkoska, K. Galić, *et al.*, The effect of barrier properties of polymeric films on the shelf-life of vacuum packaged fresh pork meat, *Meat Sci.*, 2019, **158**, 107880, DOI: 10.1016/j.meatsci.2019.107880.

67 P. Kaewprachu, C. Ben Amara, N. Oulahal, *et al.*, Gelatin films with nisin and catechin for minced pork preservation, *Food Packag. Shelf Life*, 2018, **18**, 173–183, DOI: 10.1016/j.fpsl.2018.10.011.

68 S. Stella, D. Garavaglia, G. Francini, V. Viganò, C. Bernardi and E. Tirloni, Evaluation of the weight loss of raw beef cuts vacuumpackaged with two different techniques, *Ital. J. Food Saf.*, 2019, **8**(4), 184–187, DOI: 10.4081/ijfs.2019.8111.

69 E. Huff-Lonergan and S. M. Lonergan, Mechanisms of water-holding capacity of meat: The role of postmortem biochemical and structural changes, *Meat Sci.*, 2005, **71**(1), 194–204, DOI: 10.1016/j.meatsci.2005.04.022.

70 Z. A. Nur Hanani, F. Reich, T. Tolksdorf, H. Siemen and N. Bandick, Monitoring the effect of active packaging films with silver-kaolinite using different packaging systems on the quality of beef meat, *Heliyon*, 2022, **8**(10), e11019, DOI: 10.1016/j.heliyon.2022.e11019.

71 P. B. Pathare, U. L. Opara and F. A. J. Al-Said, Colour Measurement and Analysis in Fresh and Processed Foods: A Review, *Food Bioprocess Technol.*, 2013, **6**(1), 36–60, DOI: 10.1007/s11947-012-0867-9.

72 M. L. Henriott, N. J. Herrera, F. A. Ribeiro, *et al.*, Impact of myoglobin oxygenation state prior to frozen storage on color stability of thawed beef steaks through retail display, *Meat Sci.*, 2020, **170**, 108232, DOI: 10.1016/j.meatsci.2020.108232.

73 J. B. Hutchings, *Food Colour and Appearance*, Springer US, 1999. DOI: 10.1007/978-1-4615-2373-4.

74 P. A. V. Freitas, C. González-Martínez and A. Chiralt, Using rice straw fractions to develop reinforced, active PLA-starch bilayers for meat preservation, *Food Chem.*, 2023, **405**, 134990, DOI: 10.1016/j.foodchem.2022.134990.

75 H. K. Park, Evaluation of dry rehydratable film method for detection of coliform bacteria and Escherichia coli, *Korean J. Food Nutr.*, 2009, **22**(4), 696–700.

76 Y. Y. Qin, J. Y. Yang, H. B. Lu, *et al.*, Effect of chitosan film incorporated with tea polyphenol on quality and shelf life of pork meat patties, *Int. J. Biol. Macromol.*, 2013, **61**, 312–316, DOI: 10.1016/j.ijbiomac.2013.07.018.

77 F. Xu, C. Wang, H. Wang, Q. Xiong, Y. Wei and X. Shao, Antimicrobial action of flavonoids from Sedum aizoon L. against lactic acid bacteria in vitro and in refrigerated fresh pork meat, *J. Funct. Foods*, 2018, **40**, 744–750, DOI: 10.1016/j.jff.2017.09.030.

78 European Commission, Commission Regulation (EC) No 2073/2005 of 15 November 2005 on microbiological criteria for foodstuffs, *Off. J. Eur. Union*, 2005, **338**, 1–26.

79 Y. Xiong, M. Chen, R. D. Warner and Z. Fang, Incorporating nisin and grape seed extract in chitosan-gelatine edible coating and its effect on cold storage of fresh pork, *Food Control*, 2020, **110**, 107018, DOI: 10.1016/j.foodcont.2019.107018.